

# We are IntechOpen, the world's leading publisher of Open Access books Built by scientists, for scientists

6,300

Open access books available

171,000

International authors and editors

190M

Downloads

Our authors are among the

154

Countries delivered to

TOP 1%

most cited scientists

12.2%

Contributors from top 500 universities



WEB OF SCIENCE™

Selection of our books indexed in the Book Citation Index  
in Web of Science™ Core Collection (BKCI)

Interested in publishing with us?  
Contact [book.department@intechopen.com](mailto:book.department@intechopen.com)

Numbers displayed above are based on latest data collected.  
For more information visit [www.intechopen.com](http://www.intechopen.com)



# Kinetics of Drying Medicinal Plants by Hybridization of Solar Technologies

*Margarita Castillo Téllez, Beatriz Castillo Téllez,  
José Andrés Alanís Navarro, Juan Carlos Ovando Sierra  
and Gerardo A. Mejia Pérez*

## Abstract

Historically, medicinal plants have always had an important place in medicine. Medicinal plants processing represents a great challenge, due to their compounds sensitive to the environmental conditions that surround and degrade them. Mostly of these plants require to be dry to preserve its safety and medicinal properties; therefore, for proper drying, it is necessary to use sustainable devices that protect the desirable characteristics of plants from direct radiation. In this work, the kinetics of dehydration of three medicinal plants are presented in an indirect solar dryer. In addition, the experimental results were adjusted to nine mostly used models, to estimate the drying conditions required to achieve a desired final moisture content. Modified Page and Page were the models with better fit to experimental results. Furthermore, a computational simulation of temperature evolution and distribution inside the dryer is presented. These results agree with those obtained experimentally.

**Keywords:** medicinal plants, indirect solar drying, mathematical model, colorimetric study, computational analysis

## 1. Introduction

The knowledge of medicinal plants extends to any part of the world where man has traditionally needed them to cure his illnesses. Thus, a mixture of magic and religion, combined with necessity and chance, trial and error, the passage of different cultures has created a whole knowledge of plant remedies that has been the basis of modern medicine [1]. However, many studies have been performed to test if they are truly effective and, as a result of these studies, the therapeutic use of many medicinal plants as substitutes for pharmaceutical medicines has been applied successfully to cure or relieve diseases [2].

According to the WHO, herbal medicines include herbs, herbal material, preparations, and herbal products, which contain as active ingredients parts of plants or other plant materials, and their use is well established and widely recognized as safe and effective [3].

It has been shown in studies and reviews that medicinal plants have various properties that cure, for example, anticancer and antiviral activities [4],

antidiabetic properties [5], anti-dengue activities [6], infertility problems [7], contusion and swelling, plants that improves learning and retrieval processes, and facilitates memory retention, to treat Alzheimer disease, hepatitis, significant anesthetic activity, antiarrhythmic action and even anti-obesity [8–11].

In this work, three medicinal plants were selected, which for many years have been considered important because of the amount of medicinal properties they possess and because the literature has corroborated their effectiveness in various treatments.

One of the most used plants for medical purposes in the world is *Annona* (*Annona muricata* L.) which is a comestible tropical fruit widely cultivated through the world [12]. The roots of these species are used for their antiparasitic and pesticidal properties. Intensive chemical investigations of the leaves and seeds of this plant have resulted in the isolation of a great number of bioactive compounds which were found to display interesting biological including antitumor, anticancer, antiparasitic and pesticidal properties [13, 14]. Literature revealed that *Annona* fruit extracts possess antioxidant properties and were able to inhibit enzymes relevant to type-2 diabetes and hypertension [15].

On the other hand, also, *Moringa oleifera*, native to India, is fully utilized for its high nutritive values. The leaves have many minerals and vitamins and are utilized to treat malnutrition, to increase breast milk production in women, and as a powerful antioxidant, anticancer, anti-inflammatory, antidiabetic, and antimicrobial agent. There is literature that provides relaxing inducing properties [16–19].

Finally, *Cymbopogon*. It is native to Asia and grows in tropical and subtropical regions [19]. There are many medicinal uses of *Cymbopogon* because it has many functional properties. The leaves and the essential oil are consumed to help with dyspeptic disorders, colds, nervous conditions, and exhaustion. It was found that they have a potential anticarcinogenic action [20] and antimicrobial, sedative, spasmolytic, and carminative effects. It has also been shown to have antifungal, anti-inflammatory, antimutagenic, antimalarial, antinociceptive, antibacterial, and cholesterol reduction effects [21–26].

The preparation of medicinal plants depending on its use, is very important to reach the maximum potential action in the human body, but the most frequently performed preparation is drying the leaves and using them in teas or distilling them to produce essential oils.

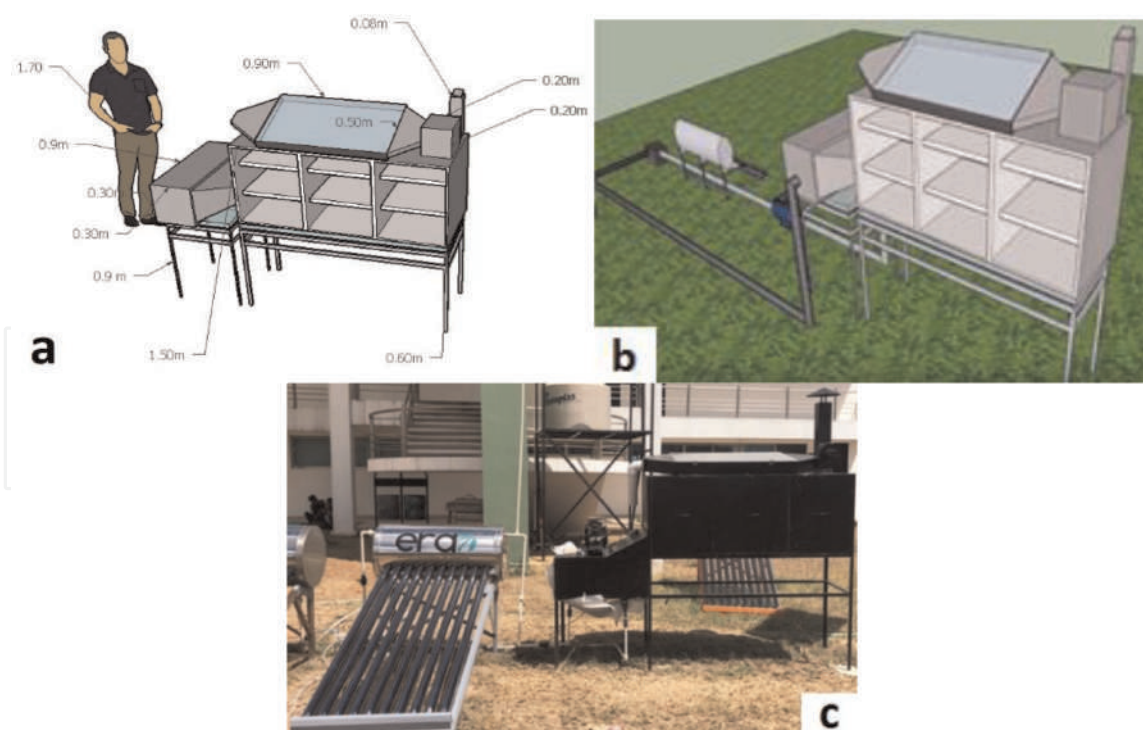
Drying is fundamentally defined the elimination of the majority of plant moisture content, permitting the prevention of enzymatic and microbial activity and therefore preserving the product for extended shelf life. Moreover, the properties of medicinal plants are determined by their moisture content. Mostly of its preparation needs the elimination of water. Consequently, adequate dryers are very important, including control of temperature, velocity, and humidity values, and in many cases, direct solar radiation is forbidden to provide a rapid reduction in the moisture content without affecting the quality of medicinal plants. Drying process aids the marketing of plants, because drying allows to improve the distribution of the plants since it reduces both the weight and the volume, reducing the transport and storage needs [27].

Therefore, in this work, an indirect solar dehydrator was designed, with which the plant is protected from its high sensitivity to high temperatures and solar radiation.

## 2. Experimental study

### 2.1 Construction of the solar dryer

In this study, an indirect solar dryer type tunnel with solar technology hybridization was constructed (**Figure 1**): This dryer is hermetically sealed and is composed of three front sections. Each section contains two trays with a metallic



**Figure 1.**  
 Tunnel-type solar dryer: (a) main measurements and location of trays, (b) location of solar heater and solar air collector, (c) the indirect solar dryer in operation. Source: Own elaboration.

mesh to support the hot air flow evenly. Each tray has a separation of 20 cm, as shown in **Figure 1a**. The drying chamber is connected to a solar water heater by a hopper, which drives preheated air inside, supported by a heat exchanger. Additionally, the dryer has a solar air collector installed at the top. This collector contains a fan that extracts the ambient air through the interior and directs it, with an increase in temperature, to the interior of the drying chamber (**Figure 1b**). The solar dryer has a 1/2 hp. motor that extracts ambient air into the solar air collector and an electric pump that recirculates the water in the solar heater, both systems work with a 280 W solar panel. **Figure 1c** shows the indirect solar dryer in operation.

## 2.2 Measuring instruments

In order to ensure the reliability of the experimental results, different measuring equipment were used at the different stages of the experimentation; Boeco mark food moisture measurement scale, model BMA150, with an accuracy of  $\pm 1$  mg (0.001%) was used to determine the initial and final humidity of the leaves. The leaf sample of approximately 1.5 g was cut and placed in the analyzer. Water activity in the leaves under study was measured by a mark team Rotronic HygroPalm, with an accuracy of  $\pm 0.01\%$  mg. The mean of three measurements was reported at a room temperature of  $24.5 \pm 1^\circ\text{C}$ . The temperature and humidity inside the drying chambers were measured using a Brannan thermo-hygrometer with temperature and relative humidity accuracy of  $\pm 1^\circ\text{C}$  and  $\pm 3\%$ , respectively. The weight of the samples was measured using a Boeco weighing scale, model BPS40plus, which have an accuracy of  $\pm 0.001$  g.

The weather parameters were monitored by the weather station located in the Faculty of Engineering of the Autonomous University of Campeche, which consists of a LI-COR Pyranometer, with which the global solar irradiance was measured; the accuracy is Azimuth:  $< \pm 1\%$  on  $360^\circ$  to  $45^\circ$  of elevation. The relative humidity, ambient temperature, and wind velocity and direction were measured by NG Systems mark equipment, model RH-5X (accuracy  $\pm 3\%$ ),



110S (accuracy  $\pm 1.1^\circ\text{C}$ ), Series #200P (accuracy  $\pm 3^\circ$ ), and P2546C-OPR (accuracy  $\pm 0.3 \text{ m/s}$ ), respectively.

### 2.3 Drying process and experimental setup

In this study, the kinetics of drying medicinal plants using an indirect solar dryer were analyzed experimentally to determine optimal operating conditions, evaluating the possibility of the integration of solar technologies in solar food drying. Samples of fresh leaves were cut from plantings on agricultural land, in the month of March 2019, in the city of Campeche, Campeche, Mexico. The experimental study was carried out from March 4 to April 26. The branches were cut, and the leaves were separated and selected to obtain a homogeneous group, based on maturity, color, freshness, and size. They were washed and weighed, and the width, length, and thickness were measured.

To analyze the initial and final humidity in the plants, the leaf sample of approximately 1.5 g was cut and placed in the analyzer. Water activity ( $a_w$ ) is a parameter that determines the stability of the food with respect to the ambient humidity. It was measured for both fresh and dried leaves before and after the drying process using portable water activity meter.

The plants that were selected for experimentation were *Moringa oleifera*, *Annona muricata* L., and *Cymbopogon citratus*. *Moringa oleifera*, is a plant that has generated great interest in recent years because of its attributed medicinal properties [28], contains more than 90 nutrients, different antioxidants, and all the 8 essential amino acids [29]. The main medicinal property of *Cymbopogon Citratus* is to be anti-inflammatory and antioxidant due to polyphenols, it contains, so it is used in cases of cancer and to combat arthritis among other properties [30].

Fresh and dried leaves were placed on a flat surface, and the colorimeter was placed on the leaves to measure color values. For each sample, the measurements were replicated four times, obtaining in each measurement the values  $L^*$  (luminance),  $a^*$  (brownness), and  $b^*$  (darkness) [31].

The total color change ( $\Delta E$ ) was the parameter considered for the overall color difference evaluation, between a dried sample and the fresh leaf [32]:

$$\Delta E = \sqrt{(L_o - L)^2 + (a_o - a)^2 + (b_o - b)^2} \quad (1)$$

### 2.4 Mathematical modeling

In order to observe the drying behavior of medicinal plants, the moisture ratio against the drying time was plotted. The dry-based moisture ratio during the drying process was calculated using the following equation [33]:

$$MR_{db} = \frac{M_t}{M_0} \quad (2)$$

where  $M_t$  and  $M_0$  are the moisture content in time  $t$  and the initial moisture content (kg water/kg dry matter), respectively.

#### 2.4.1 Adjusting experimental drying curves

The experimental moisture-versus-time ratio was adjusted by nonlinear regression to nine thin-layer drying models (**Table 1**) for each drying kinetic of the

| Model name           | Model equation                       | Reference |
|----------------------|--------------------------------------|-----------|
| Newton               | $MR = \exp(-kt)$                     | [35]      |
| Page                 | $MR = \exp(-kt^n)$                   | [36]      |
| Modified page        | $MR = \exp(-(kt)^n)$                 | [37]      |
| Henderson and Pabis  | $MR = a \exp(-kt)$                   | [38]      |
| Logarithmic          | $MR = a \exp(-kt) + c$               | [39]      |
| Two-term             | $MR = a \exp(-k_0t) + b \exp(-k_1t)$ | [40]      |
| Two-term exponential | $MR = a \exp(-kt) + (1 - a)$         | [41]      |
| Wang and Singh       | $MR = 1 + at + bt^2$                 | [42]      |
| Weibull              | $MR = \exp[-(t/b)^\alpha]$           | [43]      |

Source: Own elaboration.

**Table 1.**  
*Mathematical models used to predict the drying kinetics of medicinal plants.*

medicinal plants. The criteria used to select the model that best fit the data experimental were the coefficient of determination ( $R^2$ ) and the root of the mean square error (RMSE), considering that values of  $R^2$  superior to 0.95 RMSE values below 0.06 indicate good fit [34]. In addition, a lower value of  $X^2$  is considered as indicative of better fit. The adjustment was solved for the calculation of the different parameters involved in the selected fit models using the DataFix software version 9.1.

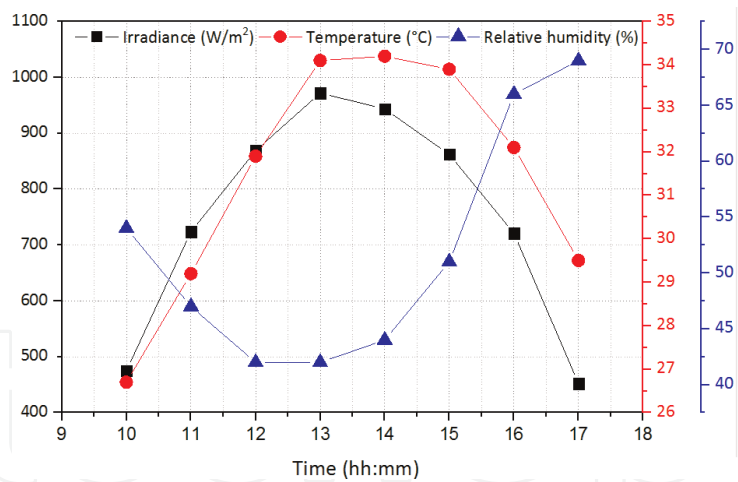
### 3. Results and discussion

Moisture tests were performed on fresh and dehydrated leaves; in all cases, the average initial humidity was 73.8%, the maximum readings were 79.58%, and the minimum readings were 68.2%. These readings agree with those reported in the literature (Banchero, Carballo, & Telesca, 2007). The initial average  $a_w$  was 0.976, the minimum measured was 0.96, while the maximum was 0.98. The average final  $a_w$  in all cases was 0.44, the minimum measured reading was 0.33, and the maximum was 0.58. The final  $a_w$  values indicate that there is no possibility of microbial growth in the dehydrated product obtained [44].

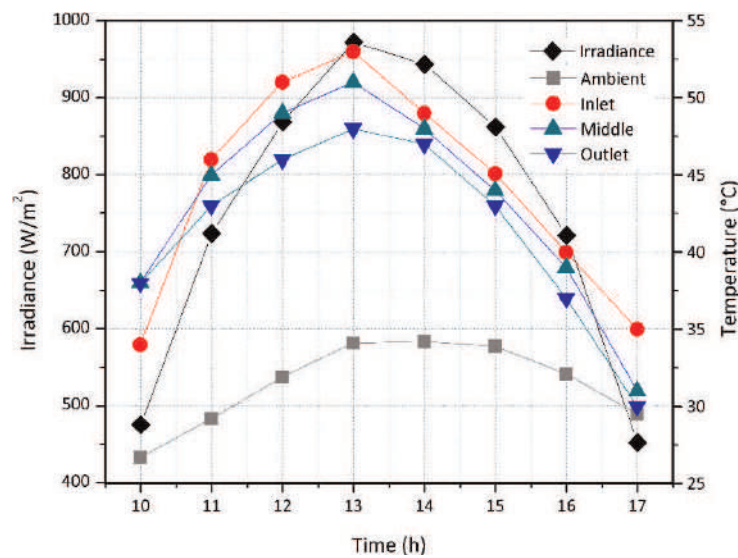
#### 3.1 Weather conditions

**Figure 2** shows the change in the weather parameters during the test period with three sunny days. As can be seen, a maximum solar global irradiance of  $952 \text{ W/m}^2$  was achieved, with the average maximum values ranging between 874 and  $962 \text{ W/m}^2$ . The average ambient temperature varied of  $30^\circ\text{C}$  y  $35.7^\circ\text{C}$ . On the other hand, the minimum RH (relative humidity) ranged between 44 and 46%; the maximum average on the test days ranged between 60 and 81%.

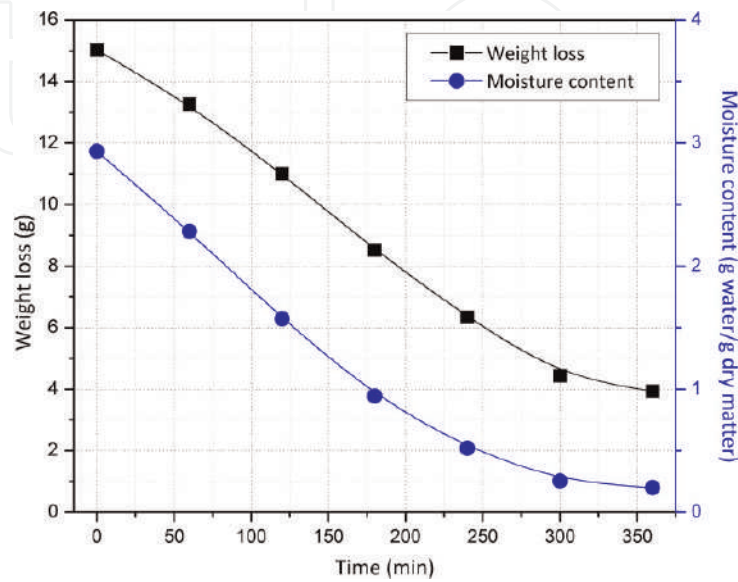
**Figure 3** shows the temperatures inside the drying chamber, solar radiation, and the ambient temperature during the hours with the highest solar incidence on the selected day as an example. The drying chamber consists of three sections with similar temperatures. The highest temperature reaches  $50.7^\circ\text{C}$ .



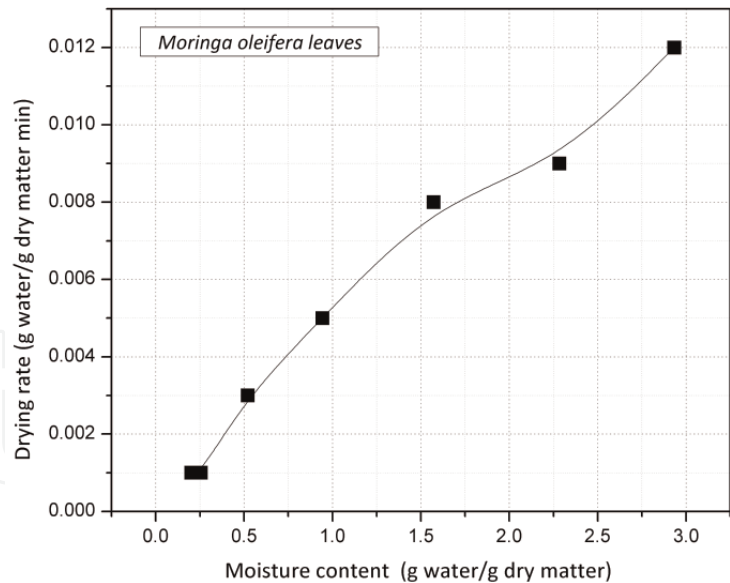
**Figure 2.**  
Average solar irradiance, ambient temperature, and relative humidity. Source: Own elaboration.



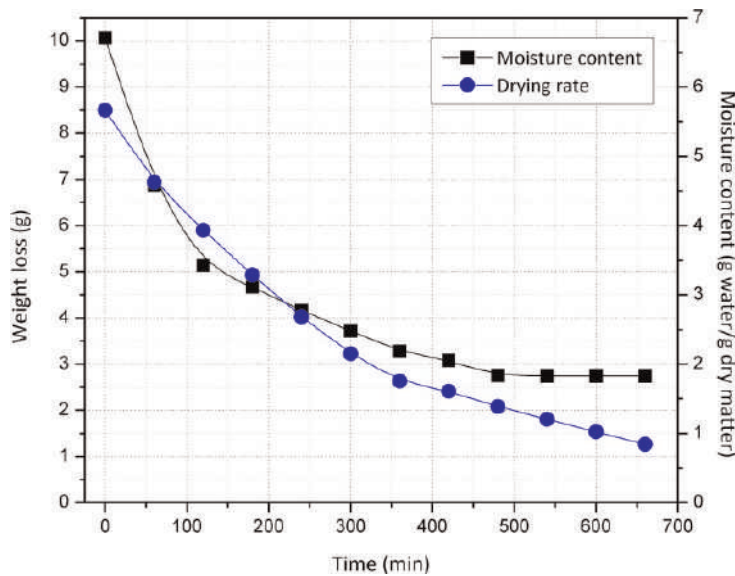
**Figure 3.**  
Solar irradiance variation and temperature inside the drying chamber of the tunnel solar dryer. Source: Own elaboration.



**Figure 4.**  
Weight loss and moisture content depending on the drying time for *Moringa oleifera* leaves. Source: Own elaboration.



**Figure 5.**  
Drying rate as function of moisture content for a *Moringa oleifera* leaves. Source: Own elaboration.



**Figure 6.**  
Weight loss and moisture content depending on the drying time for *Annona muricata* leaves. Source: Own elaboration.

### 3.2 Solar drying kinetics

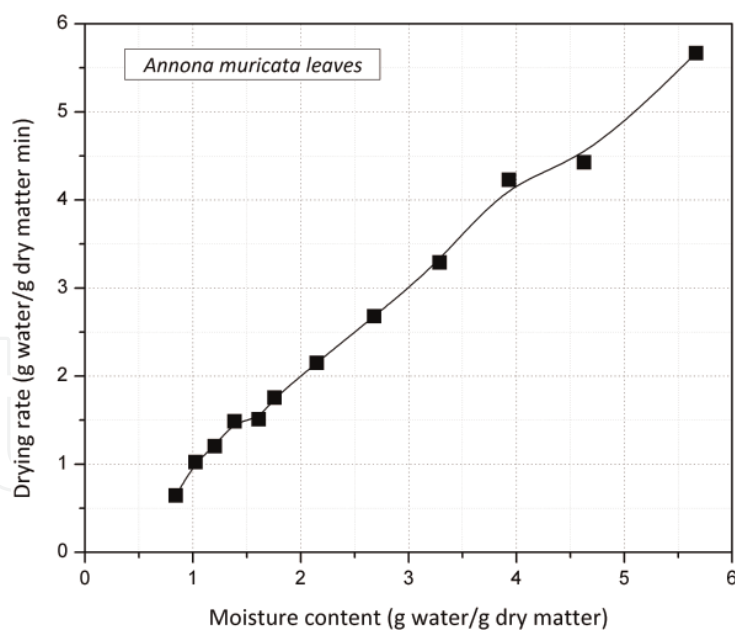
#### 3.2.1 *Moringa oleifera* leaves

The weight loss stabilized upon reaching this sample 3.9 g; the final drying time was 360 min. It can be seen in **Figure 4** that the moisture content started at 2.93 g water/g dry matter, ending between 0.201 and 0.256. **Figure 5** shows the moisture content as a function of the drying rate; in this case no constant rate period was observed. The highest drying rate was found with 0.012 g water/g dry matter minute.

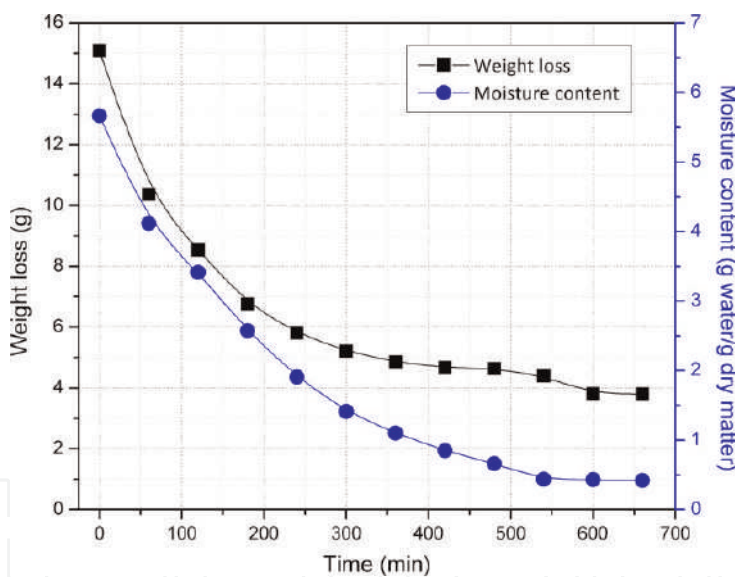
#### 3.2.2 *Annona muricata* leaves

In the case of *Annona muricata* leaves, the total drying time was 500 min, (**Figure 6**); the initial moisture content was 5.667 g water/g dry matter, reaching a





**Figure 7.**  
Drying rate as function of moisture content for an *Annona muricata* leaves. Source: Own elaboration.

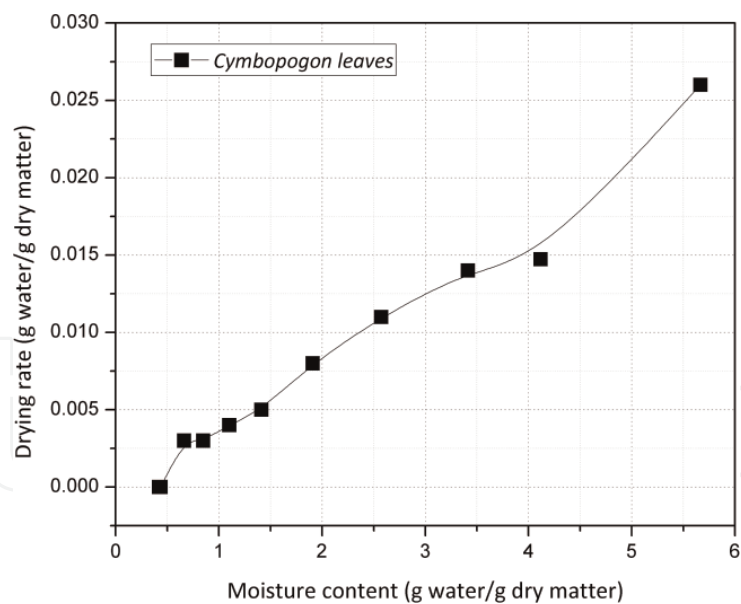


**Figure 8.**  
Weight loss and moisture content depending on the drying time for *Cymbopogon* leaves. Source: Own elaboration.

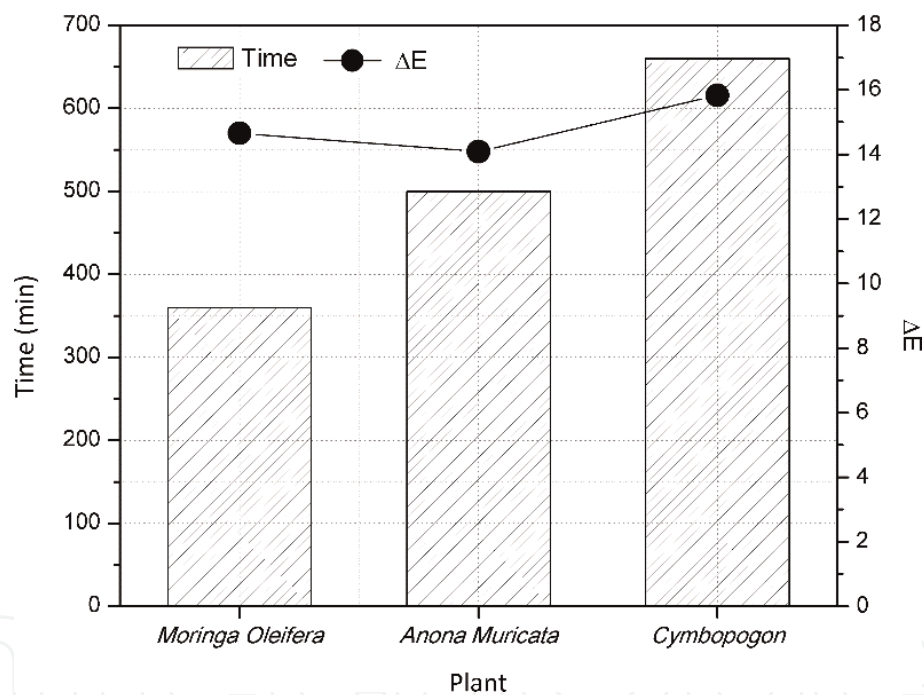
final moisture content between 0.843 g water/g dry matter and 1.204 g water/g dry matter. Reaching a final drying rate between 0.643 g water/g matter dry minute and 1.024 g water/g matter dry minute, the final weight of the sample was 2.7 g (see **Figure 7**).

### 3.2.3 *Cymbopogon*

As can be seen in **Figure 8**, the drying kinetics of the *Cymbopogon* sample stabilized in 660 min. The initial moisture content was 5.66 g water/g dry matter. The final moisture content was between 0.421 and 0.435. **Figure 9** shows that the highest drying rate was 0.026 g water/g dry matter min.



**Figure 9.**  
Drying rate as function of moisture content for a *Cymbopogon* leaves. Source: Own elaboration.



**Figure 10.**  
Relationship between final drying time and  $\Delta E$  in dehydrated leaves. Source: Own elaboration.

### 3.3 Colorimetric analysis

Color is a primary characteristic perceived by the consumer of a product and plays an important role in food. The color of food is often an indication of the nutrients it contains. In addition, the color of a processed product is expected to be as similar as possible to fresh ones [45].

**Table 2** shows the values obtained from  $L^*$ ,  $a^*$ , and  $b^*$ , in the medicinal plants studied in fresh and dry.

An insignificant variation in the parameters  $L^*$ ,  $a^*$ , and  $b^*$  obtained in the plants studied before and after the drying process can be seen in **Table 2**. This can be corroborated in **Figure 10**, in which  $\Delta E$  is analyzed. The main reason for this color preservation is the protection against solar irradiation of the solar tunnel dryer, so

dehydrated plants are kept more similar to fresh ones. For this reason, it is preferable to dry in a closed and controlled environment, which is consistent with studies of Helvaci et al. [46].

It is important to note that in all cases the values of  $L^*$ ,  $a^*$ , and  $b^*$  decreased; this means that as the temperature increased (the three sections of the drying chamber reached up to 50.7°C). There was a tendency toward gray colors, a decrease in red colors (more brown), and an increase in yellow colors; these results agree with data reported by Bhardwaj et al. [47].

3.4 Computational analysis

Computational simulation is performed by using of a free software called Energy2D [48]. Simulation consists of temperature dependence upon time at dif-

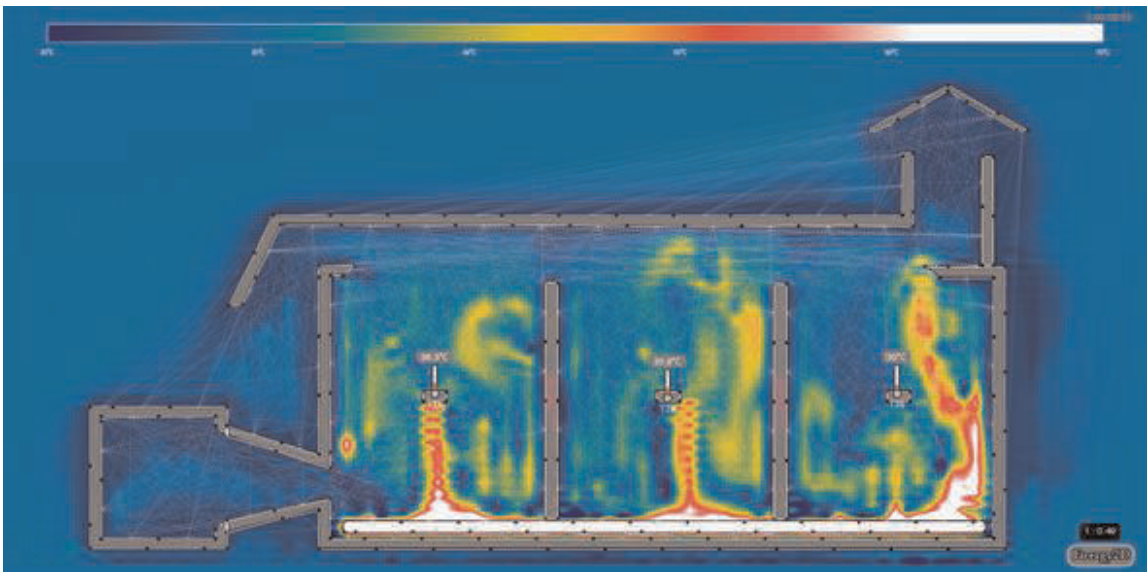





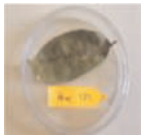
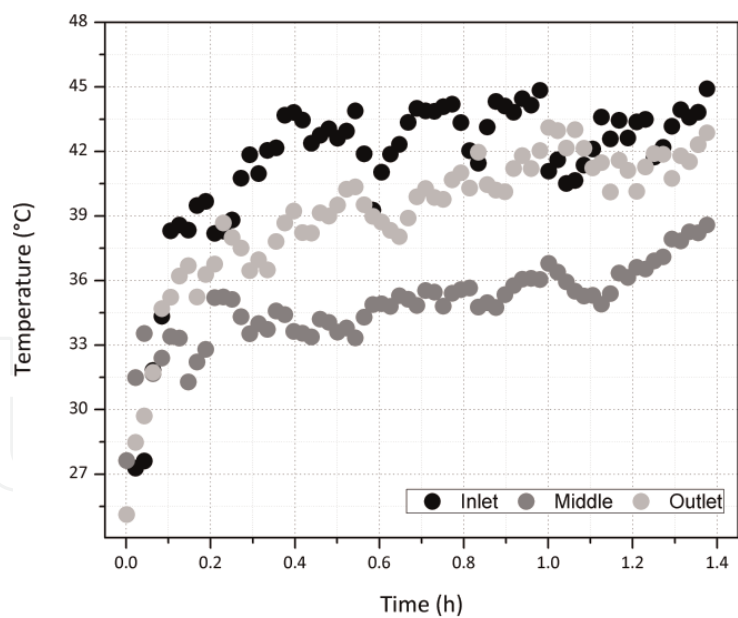


Figure 11. Thermal behavior simulation of the dehydrator. Source: Own elaboration.

| L*, a*, b* values and drying                       | Medicinal plants  |   |   |
|--|---|---|---|
|  | <i>Moringa oleifera</i>   | <i>Cymbopogon</i>   | <i>Annona muricata</i>  |
| Fresh leaves<br>L*, a*, b* values                  | <br>L: 50.28<br>a: -6.76<br>b: 35.75 | <br>L: 50.2<br>a: -7.87<br>b: 21.81 | <br>L: 45.53<br>a: -8.41<br>b: 27.58 |
| Dehydration with tunnel dryer<br>L*, a*, b* values | <br>L: 40.4<br>a: -2.61<br>b: 25.75  | <br>L: 41.27<br>a: 1.85<br>b: 13.14 | <br>L: 37.02<br>a: -5.24<br>b: 16.81 |

Source: Own elaboration.

Table 2. Values obtained from  $L^*$ ,  $a^*$ ,  $b^*$  (fresh and dried) in the medicinal plants studied.

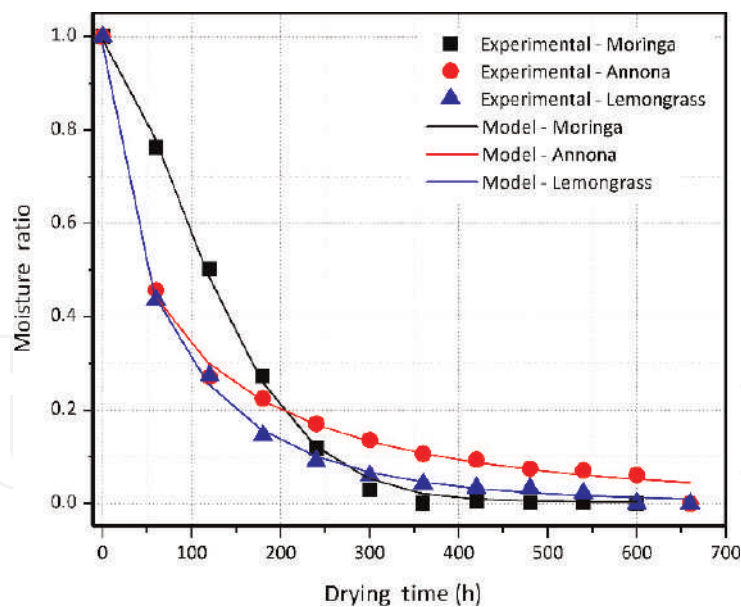


**Figure 12.**  
Graph of thermal behavior simulation of the dehydrator. Source: Own elaboration.

|               |                                |        |
|---------------|--------------------------------|--------|
| Annona        |                                |        |
| Model         | Coefficients and fit parameter | Value  |
| Modified page | k                              | 0.0116 |
|               | n                              | 0.5685 |
|               | R <sup>2</sup>                 | 0.9941 |
|               | RMSE                           | 0.0199 |
|               | X <sup>2</sup>                 | 0.0005 |
| Cymbopogon    |                                |        |
| Model         | Coefficients and fit parameter | Value  |
| Modified page | k                              | 0.0369 |
|               | n                              | 0.7545 |
|               | R <sup>2</sup>                 | 0.9988 |
|               | RMSE                           | 0.0092 |
|               | X <sup>2</sup>                 | 0.0001 |
| Moringa       |                                |        |
| Model         | Coefficients and fit parameter | Value  |
| Page          | k                              | 0.0067 |
|               | n                              | 1.5616 |
|               | R <sup>2</sup>                 | 0.9987 |
|               | RMSE                           | 0.0119 |
|               | X <sup>2</sup>                 | 0.0001 |

Source: Own elaboration.

**Table 3.**  
Results of regression analysis of the best adjusted models.



**Figure 13.**  
*Experimental versus mathematical model. Source: Own elaboration.*

ferent zones. For the temperature evolution across time, thermal conduction and convection simulation mode was selected. For accurate results, also the thermal and optical properties of each material were chosen. The complete procedure of simulation can be found in Ref. [49]. In **Figure 11**, the thermal behavior of the dehydrator is shown and can be distinguished into three zones: left, middle, and right. Maximum reached values of temperature sensors, at the left, middle, and right zones were 45.2, 38.8, and 44.7°C, respectively, while its averages were about 41.4, 34.9, and 39.2°C, correspondingly. The temporal fluctuation of temperature is depicted in **Figure 12**.

The temperatures reached in the dryer with the hybridization of solar technologies remained stable during most of the day, with a variation between 45 and 50°C (**Figures 3 and 12**), which, as reported in the literature reviewed, are optimal to prevent the loss of important properties in vegetables and medicinal plants [46, 50].

### 3.5 Mathematical modeling

#### 3.5.1 Adjusting experimental drying curves

The drying kinetics obtained experimentally in the medicinal plants were adjusted using the nine drying models mentioned in **Table 1**. **Table 3** presents the model that best fit for each drying condition. These models had the highest  $R^2$  values as shown in **Table 2**.

Estimates of the statistical parameter for all experimental conditions showed that  $R^2$  values ranged from 0.991 to 0.9988, indicating a good fit [34]. Therefore, these models adequately predict the selected plant drying kinetics. From the data, Modified Page model was the most suitable for describing drying processes of *Annona* and *Cymbopogon* drying conditions and Page for *Moringa* (see **Figure 13**).

## 4. Conclusion

*Moringa oleifera*, *Cymbopogon*, and *Annona muricata* have antioxidant, anticancer, anti-inflammatory, antidiabetic, antimicrobial, and many more positive effects



in the human body. The drying kinetics of this plants were analyzed using a constructed indirect solar dryer type tunnel. It was possible to obtain optimum temperatures for drying (45–50°C), and drying times were significantly reduced by keeping these temperatures constant for a longer time throughout the day.

The quality of the plants at the end of drying was confirmed when obtaining average  $a_w$  values of 4.4. The average final moisture content of the three medicinal plants varied between 0.8 and 1.5 g water/g dry matter. The moisture ratio was fitted to nine thin-layer drying mathematical models to select a suitable drying curve. The Modified Page and Page models showed the best fit to the experimental results. The time required to reach the equilibrium moisture content in all experiments varied between 250 and 350 min. The superior efficiency of the dryer allows a reduction of the important drying costs. This technology would allow agricultural producers to reduce costs while contributing to the improvement of the environment.

## Author details

Margarita Castillo Téllez<sup>1\*</sup>, Beatriz Castillo Téllez<sup>2</sup>, José Andrés Alanís Navarro<sup>3</sup>, Juan Carlos Ovando Sierra<sup>1</sup> and Gerardo A. Mejia Pérez<sup>2</sup>


1 Facultad de Ingeniería, Universidad Autónoma de Campeche, Campus V, Unidad Habitacional Siglo XXIII por Avenida Ing. Humberto Lanz Cárdenas, Campeche, Mexico

2 Centro Universitario del Norte, Universidad de Guadalajara, Colotlán, Jalisco, México

3 Energy Department, Polytechnic University of Guerrero's State, Puente Campuzano, Guerrero, México

\*Address all correspondence to: [mcastill@uacam.mx](mailto:mcastill@uacam.mx)

## IntechOpen

© 2019 The Author(s). Licensee IntechOpen. This chapter is distributed under the terms of the Creative Commons Attribution License (<http://creativecommons.org/licenses/by/3.0>), which permits unrestricted use, distribution, and reproduction in any medium, provided the original work is properly cited. 

## References

- [1] Pérez Ortega G, González Trujano E. Plantas medicinales contra la ansiedad. Universidad del Zulia. 2015; **22**(3):68-75
- [2] Sofowora A, Ogunbodede E, Onayade A. The role and place of medicinal plants in the strategies for disease prevention. African Journal of Traditional, Complementary, and Alternative Medicines. 2013;**10**(5): 210-229
- [3] WHO Global Report on Traditional and Complementary Medicine 2019. Geneva: World Health Organization; 2019. Licence: CC BY-NC-SA 3.0 IGO
- [4] Rastogi RP, Dhawan BN. Anticancer and antiviral activities in Indian medicinal plants: A review. Drug Development Research. 1990;**19**(1):1-12
- [5] Surya S, Salam AD, Tomy DV, Carla B, Kumar RA, Sunil C. Diabetes mellitus and medicinal plants: A review. Asian Pacific Journal of Tropical Disease. 2014;**4**(5):337-347
- [6] Abd Kadir SL, Yaakob H, Mohamed Zulkifli R. Potential anti-dengue medicinal plants: A review. Journal of Natural Medicines. 2013;**67**(4):677-689
- [7] Nantia EA, Moundipa PF, Monsees TK, Carreau S. Les plantes médicinales dans le traitement de l'infertilité chez le mâle: Mise au point. Andrologie. 2009;**19**(3):148-158
- [8] Marshall E. Health and wealth from medicinal aromatic plants. FAO; 2011. pp. 1-73
- [9] Johnson RK et al. Dietary sugars intake and cardiovascular health: A scientific statement from the American Heart Association. Circulation. 2009; **120**(11):1011-1020
- [10] Zhu DY, Bai DL, Tang XC. Recent studies on traditional Chinese medicinal plants. Drug Development Research. 1996;**39**(2):147-157
- [11] Hasani-Ranjbar S, Jouyandeh Z, Abdollahi M. A systematic review of anti-obesity medicinal plants: An update (Provisional abstract), " Database of Abstracts of Reviews of Effects. 2013;**1**:28
- [12] McCarty MF. ACE inhibition may decrease diabetes risk by boosting the impact of bradykinin on adipocytes. Medical Hypotheses. 2003;**60**(6): 779-783
- [13] Gleye C, Laurens A, Hocquemiller R, Olivier L, Laurent S, Cavé A. Cohibins A and B, acetogenins from roots of *Annona Muricata*. Phytochemistry. 1997;**44**(8):1541-1545
- [14] Rady I et al. Anticancer properties of Graviola (*Annona muricata*): A comprehensive mechanistic review. Oxidative Medicine and Cellular Longevity. Hindawi; 2018. pp. 39. Article ID: 1826170
- [15] Adefegha SA, Oyeleye SI, Oboh G. Distribution of phenolic contents, antidiabetic potentials, antihypertensive properties, and antioxidative effects of Soursop (*Annona muricata* L.) fruit parts in vitro. Biochemistry Research International. 2015;**2015**
- [16] Saroj K, Mukherjee PK, Pal M. Studies on some psychopharmacological actions of Moringa. 1996;**10**:402-405
- [17] Perumal S, Klaus B. Antioxidant properties of various solvent extracts of total phenolic constituents from three different agroclimatic origins of drumstick tree (*Moringa oleifera* Lam.) Leaves. Journal of Agricultural and Food Chemistry. 2003;**51**(8):2144-2155
- [18] Castillo TM, Castillo TB, Viviana MME, Carlos OSJ. "Technical and

experimental study of the solar dehydration of the moringa leaf and its potential integration to the sustainable agricultural industry,” European Journal of Sustainable Development. 2018;7(3): 65-73

[19] Charles DJ. Antioxidant Properties of Spices, Herbs and Other Sources. Vol. 4. Springer; 2013. pp. 1-610

[20] qiang Zheng G, Kenney PM, Lam LKT. Potential anticarcinogenic natural products isolated from lemongrass oil and galanga root oil. Journal of Agricultural and Food Chemistry. 1993;41(2):153-156

[21] Aldawsari HM, Badr-Eldin SM, Labib GS, El-Kamel AH. Design and formulation of a topical hydrogel integrating lemongrass-loaded nanosponges with an enhanced antifungal effect: In vitro/in vivo evaluation. International Journal of Nanomedicine. 2015;10:893-902

[22] Bidinotto LT, Costa CARA, Salvadori DMF, Costa M, Rodrigues MAM, Barbisan LF. Protective effects of lemongrass (*Cymbopogon citratus* STAPF) essential oil on DNA damage and carcinogenesis in female Balb/C mice. Journal of Applied Toxicology. 2011;31(6):536-544

[23] Lee HJ, Jeong HS, Kim DJ, Noh YH, Yuk DY, Hong JT. Inhibitory effect of citral on NO production by suppression of iNOS expression and NF- $\kappa$ B activation in RAW264.7 cells. Archives of Pharmacal Research. 2008;31(3): 342-349

[24] Viuda-Martos M et al. Chemical composition and antioxidant and anti-listeria activities of essential oils obtained from some Egyptian plants. Journal of Agricultural and Food Chemistry. 2010;58(16):9063-9070

[25] Avila-Sosa R, Palou E, Jiménez Munguía MT, Nevárez-Moorillón GV,

Navarro Cruz AR, López-Malo A. Antifungal activity by vapor contact of essential oils added to amaranth, chitosan, or starch edible films. International Journal of Food Microbiology. 2012;153(1-2):66-72

[26] Monge JN, Méndez-Estrada VH. Durango (México) y Costa Rica: dos maneras contrastantes de ver la educación a distancia (Durango (Mexico) and Costa Rica: Two contrasting views of distance). Rev de Educ Distancia. 2008;28(1):1-20

[27] Calixto JB. Efficacy, safety, quality control, marketing and regulatory guidelines for herbal medicines (phytotherapeutic agents). Brazilian Journal of Medical and Biological Research. 2000;33(2):179-189

[28] Cuellar-Núñez ML, Luzardo-Ocampo I, Campos-Vega R, Gallegos-Corona MA, González de Mejía E, Loarca-Piña G. Physicochemical and nutraceutical properties of moringa (*Moringa oleifera*) leaves and their effects in an in vivo AOM/DSS-induced colorectal carcinogenesis model. Food Research International. 2018;105: 159-168

[29] Ani E, Amove J, Igbabul B. Physicochemical, microbiological, sensory properties and storage stability of plant-based yoghurt produced from bambaranut, soybean and *Moringa oleifera* seed milks. American Journal of Food and Nutrition. 2018;6(4): 115-125

[30] Luardini MA, Asi N, Garner M. Ecolinguistics of Ethno-Medicinal Plants of the Dayak Ngaju Community. Language Science; 2019

[31] T S, Al-Ismaili AM, Janitha Jeewantha LH, Al-Habsi NA. Effect of solar drying methods on color kinetics and texture of dates. Food and Bioproducts Processing. 2019;116: 227-239

- [32] Guiné Raquel PF, Barroca Maria J. Effect of drying treatments on texture and color of vegetables (pumpkin and green pepper). 2013;**90**:58-63
- [33] Shi Q, Zheng Y, Zhao Y. Mathematical modeling on thin-layer heat pump drying of yacon (*Smallanthus sonchifolius*) slices. Energy Conversion and Management. 2013;**71**:208-216
- [34] Doymaz I, Smail O. Drying characteristics of sweet cherry. Food and Bioproducts Processing. 2011;**89**(1): 31-38
- [35] Tunde-Akintunde TY. Mathematical modeling of sun and solar drying of chilli pepper. Renewable Energy. 2011; **36**(8):2139-2145
- [36] Page GE. Factors influencing the maximum rates of air drying shelled corn in thin layers. Purdue University; 1949
- [37] Diamante LM, Munro PA. Mathematical modelling of the thin layer solar drying of sweet potato slices. Solar Energy. 1993;**51**(4):271-276
- [38] Pavis S, Henderson SM. Grain drying: Temperature effect on drying coefficients. Journal of Agricultural Engineering Research. 1961;**6**:169-174
- [39] Togrul IT, Pehlivan D. Mathematical modelling of solar drying of apricots in thin layers. Journal of Food Engineering. 2002;**55**(3):209-216
- [40] Koua KB, Fassinou WF, Gbaha P, Toure S. Mathematical modelling of the thin layer solar drying of banana, mango and cassava. Energy. 2009;**34**(10): 1594-1602
- [41] Sharaf-Eldeen YI, Blaisdell JL, Hamdy MY. A model for ear corn drying. Transactions of ASAE. 1980; **23**(5):1261-1265
- [42] Wang CY, Singh RP. A single layer drying equation for rough rice. American Society of Agricultural Engineers Paper no. 78-3001; 1978
- [43] Midilli A, Kucuk H, Yapar Z. A new model for single-layer drying. Drying Technology. 2002;**20**(7):1503-1513
- [44] Jin Y, Tang J, Sablani SS. Food component influence on water activity of low-moisture powders at elevated temperatures in connection with pathogen control. Lebensmittel-Wissenschaft+ [ie und] Technologie. 2019;**112**:108257
- [45] Gonçalves EM, Pinheiro J, Abreu M, Brandão TRS, Silva CLM. Modelling the kinetics of peroxidase inactivation, colour and texture changes of pumpkin (*Cucurbita maxima* L.) during blanching. Journal of Food Engineering. 2007
- [46] Helvacı HU, Menon A, Aydemir LY, Korel F, Akkurt GG. Drying of olive leaves in a geothermal dryer and determination of quality parameters of dried product. Energy Procedia. 2019; **161**(2018):108-114
- [47] Bhardwaj AK, Kumar R, Chauhan R. Experimental investigation of the performance of a novel solar dryer for drying medicinal plants in Western Himalayan region. Solar Energy; **177**, 2019(2018):395-407
- [48] Xie C. Interactive heat transfer simulations for everyone. Physics Teacher. 2012;**50**(4):237-240
- [49] Alanís Navarro JA, Castillo Téllez M, Martínez MAR, Silvar GP, Tejeda FCM. Computational thermal analysis of a double slope solar still using Energy2D. Desalination and Water Treatment. 2019;**151**:26-33
- [50] Müller J, Heindl A. Drying of medicinal plants. Wild Relatives of Cultivated Plants in India; 2006. pp. 165-176

# We are IntechOpen, the world's leading publisher of Open Access books Built by scientists, for scientists

6,300

Open access books available

171,000

International authors and editors

190M

Downloads

Our authors are among the

154

Countries delivered to

TOP 1%

most cited scientists

12.2%

Contributors from top 500 universities



WEB OF SCIENCE™

Selection of our books indexed in the Book Citation Index  
in Web of Science™ Core Collection (BKCI)

Interested in publishing with us?  
Contact [book.department@intechopen.com](mailto:book.department@intechopen.com)

Numbers displayed above are based on latest data collected.  
For more information visit [www.intechopen.com](http://www.intechopen.com)





# Postharvest Treatment of Tropical Fruits Pineapple (*Ananas comosus*), Mamey (*Mammea americana*), and Banana (*Musa paradisiaca*) by Means of a Solar Dryer Designed

*Italo Pedro Bello Moreira, Edgar Ruperto Macías Ganchozo, Xavier Enrique Anchundia Muentes, Celio Danilo Bravo Moreira, Manuel Eduardo Anchundia Muentes, Hebert Edison Vera Delgado and Carlos Eduardo Anchundia Betancourt*

## Abstract

The objective of this research was to know the useful life of dehydrated tropical fruits based on a solar dryer designed and developed under the conditions of Calceta, Bolívar Canton of the Province of Manabí, Ecuador. The physical and chemical characteristics exhibited during the radiation dehydration process were satisfactory, in fresh pineapple from 86.36% low humidity to 21.07%, from 0.67% protein to 2.45%, and from 2.05% fiber to 3.73%; in mamey from 79.30 to 21.07%, from 0.41 to 2.55%, and from 2.50 to 4.94%; and in bananas with from 80.22 to 10.35%, from 1.27 to 2.14%, and from 0.88 to 2.42. Microbiological analyses determined the life span of the products estimated at 174, 106, and 109 days, respectively, in pineapple, mamey, and banana. As for the attributes measured with the 1–5 scale of sensory evaluation, the mean treatments of their attributes such as color, sweetness, appearance, and taste were demonstrated where bananas present better color attributes with 4.38; 4.58, sweetness; 4.58, texture; 4.68, appearance; and 4.75, flavor. Where significant diffraction can be determined relative to the calculated value  $p > 0.05$  of  $< 0.0001$ , the  $R^2$  statistic in pineapple indicates 48.0814% variability in decreasing moisture pineapple (DMP), and its correlation coefficient is equal to 0.693408; the  $R^2$  statistic in mamey indicates 55.6423% variability in decreasing moisture mamey (DMM), and its correlation coefficient is equal to 0.745938; and finally the  $R^2$  statistic in banana indicates 56.339% variability in decreasing moisture banana (DMB), and its correlation coefficient is equal to 0.750593, indicating a moderately strong relationship between variables in all cases.

**Keywords:** absorption, convective multiflash drying process (CMDf), fruit dehydration, fruit postharvest, solar energy, water activity

## 1. Introduction

In the Bolívar Canton of the city of Calceta of the Province of Manabí, Ecuador, the fruits pineapple (*Ananas comosus* (L.) Merr.), mamey (*Mammea americana* L.), and banana (*Musa paradisiaca* L.) are exuberant but due to high sugar and acid content have a limited shelf life and in many cases are wasted. Also, because these characteristics are easily adapted to conservation technologies, one of them is fundamentally dehydrated since they retain much of their taste, color, consistency, and appearance for long periods (see [1, 2]).

Sunlight from before and so far today serves to perform fruit drying as postharvest handling or conservation activity that, when purchased with other activities for the same purpose, such as chemical treatments, refrigeration, canned pre-eminence with operation, and collection even with solar drying, results in a decrease in energy expenditure spending and could therefore reach areas where other energy conveniences would not or even do not exist (see [3]).

In fruits the water present is 80.00% of its weight, for its early microbial decomposition is a definitive element. A conventional dehydrated fruit of its quality in terms of its organoleptic characteristics is lower than that of the fresh fruits from which it comes, affecting color, texture, and other peculiarities. With hot air, dehydrated fruits acquire levels of water activity ( $a_w$ ) ranging from 0.6 to 0.8; these levels retain their sensory properties, showing good firmness to microbial attacks (see [4]).

Convective multiflash drying (CMFD) is a matter that is obtained after being used to obtain crispy fruits, and it is an option to the freeze-drying process (see [5]).

The industrial-scale study, a simple convective solar drying process of pineapples such as a round or circular economy tactic for countries in progress is specified, which is paramount to the tactic offered. It built a manual solar dryer that runs in indirect heat mode; it was also changed to improve its gain. The three main elements were raised that affect the convective drying process, the drying time (270 min, 480 min), the intensity of the solar radiation ( $650 \text{ W}\cdot\text{m}^{-2}$ ,  $100 \text{ W}\cdot\text{m}^{-2}$ ), and the thickness of the cut (6–8 mm, 12–14 mm) (see [6]).

According to these instances, the aim of the research was to design and develop an empirical and practical distribution for solar dryer and drying tests to conserve the fruits and extend the shelf life, as well as organoleptic and nutritional particularities with samples of pineapple, mamey, and banana fruits in the city of Calceta, Bolívar Canton of the Province of Manabí, Ecuador.

## 2. Climate data collection

The research work was carried out from February to April 2013, in the school avenue of Calceta, Bolívar Canton, Province of Manabí, Ecuador, on the consecutive lines: South latitude  $00^{\circ}34.22'$ , west latitude  $80^{\circ}10'09.2'$ , average altitude of 22 masl, with a relative humidity of 90.00%, a temperature of  $32.8^{\circ}\text{C}$ , and a wind speed of  $8 \text{ m}\cdot\text{s}^{-1}$ , until the end of November; the respective humidity is 86.7%, the temperature is  $26^{\circ}\text{C}$ , and the speed  $1.8 \text{ m}\cdot\text{s}^{-1}$  (see [7]).

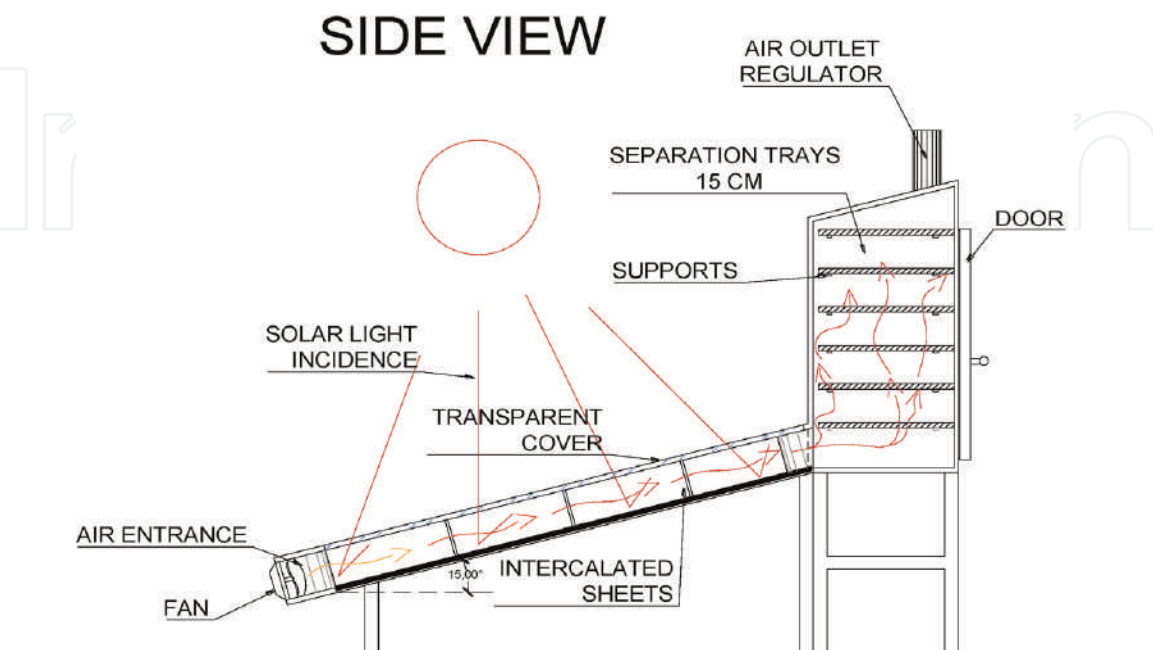
### 3. Design and construction of solar dryer

A dryer is used in heating the air by a 1 mm solar flat panel, insulated drying chamber equipped with stove where air is released for exhaust purposes. **Figure 1** describes the landscape of empirical or experimental distribution. The rustic surface of the solar collector is  $0.5 \times 0.5 \times 1$  m with a height of 0.7 m. The solar air heater is based on a folded suction plate with a dark bluish-look dyed uve (V) representation wood, as regards the exclusion of corresponding spaces on the sides as well as on the upper; the glass sheet was sealed with silicone-based material, diagonal to 15o, towards a dorsal part of the receiver (collector); a perforation was worked to carry out ventilation activities in the manner of air currents in other instances the side part, a lami was located a lami na (FV) photovoltaic to be able to understand the photoelectric effects that come from solar radiation, so with the receiver (collector) to dehydrate the fruits were stained bone white in all its accesses, covered with aluminum plate; the entrance had five ships distributed at a distance of 15 cm between each of them. The container was made of an aluminum-based wire mesh and glued to the frame inside the drying chamber. The collector outlet air enters the drying chamber at the bottom, immediately flowing into the upward orientation using the drying material. The camera was insulated from all sides except the top, the camera was tested with a fireplace for exhaust air, and the height of the fireplace was 0.25 m. These are the aspects that contemplate the construction of the solar dehydrator for the fruits (see [7]) (**Figures 2 and 3**).

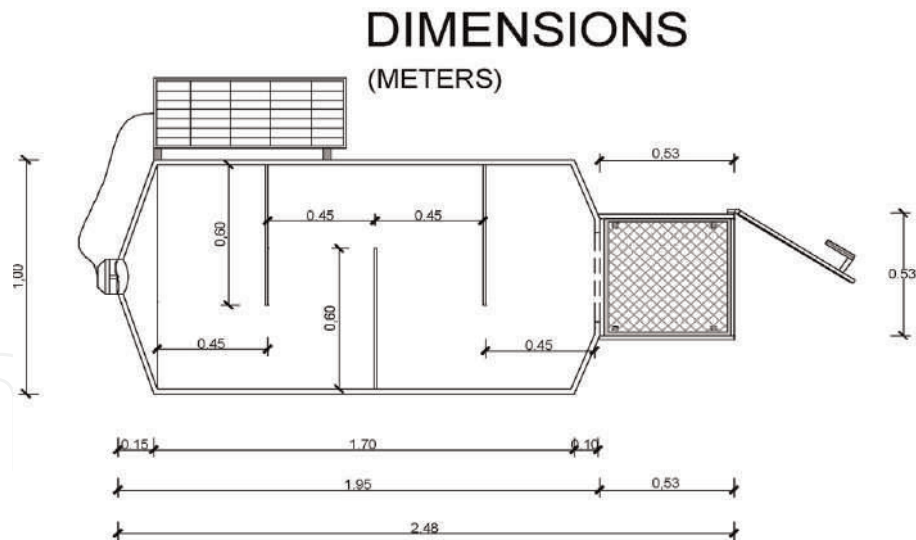
#### 3.1 System dimensioning

##### 3.1.1 Collector area calculation

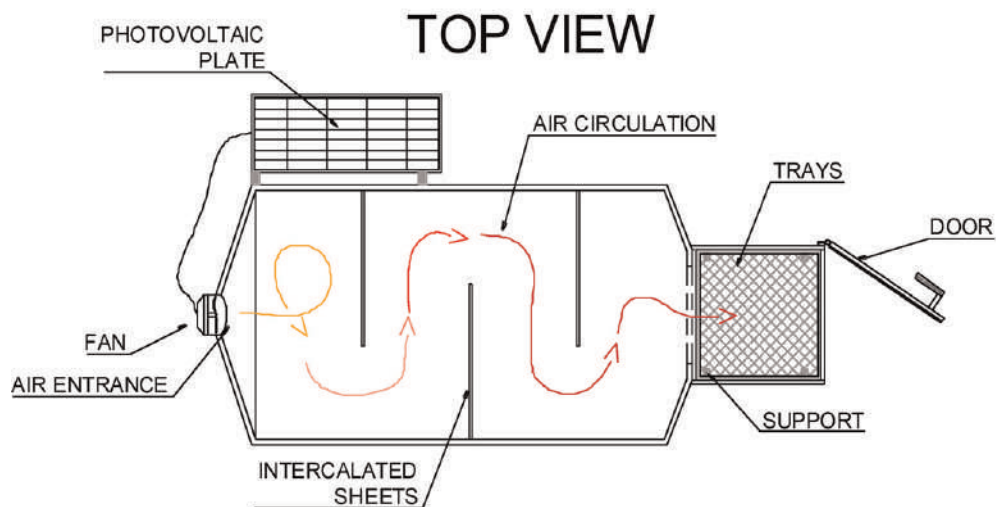
Busy strip ( $1.8 \times 1.0$ ) m.  $1.80 \text{ m}^2$ ; Global radiation on average per day  $1353 \text{ W}\cdot\text{m}^{-2}$ . Lots of temporary global units of solar radiation were calculated by manipulating a solar energy meter (Tenmar TM 207) with an accuracy of



**Figure 1.**  
*Schematic view of experimental setup with solar flat plate collector.*



**Figure 2.**  
*End-floor view.*



**Figure 3.**  
*Pair heating spray for process.*

10 W•m<sup>-2</sup>. Temperature readings were recognized every hour from 8:00 am to 6:00 pm. RTD were established at the inlet and outlet of the collector (Tin, Tout), outdoors to calculate the ambient temperature (Tamb) (see [8]).

### 3.1.2 Drying chamber

The volume of the drying chamber was established (oven example cabinet); consecutively, the average density of the fruits to be dried was  $200 \text{ Kg.m}^{-3}$ , with a mass of 4 kg;  $4/200$  to  $0.02 \text{ m}^3$ , being ten times more, a value close to 0 was obtained,  $20 \text{ m}^3$ .

### 3.1.3 Sterilization procedure

The matter is formed with preparations such as tools and components which I discuss the following:



The tools handled in the test consisted of sterilization at 180°C for 60 min according to the Medical Research Council; the chopping of the fruits was done in a sterilized part in advance rinsed with neutral soap; to quickly immerse the fruits in water with C<sub>6</sub>H<sub>8</sub>O<sub>6</sub> ascorbic acid to prevent oxidation and then fit into the dryer, start the test by placing the dehydrator; feel this part of the dryer, facing north, so that the collector takes the sun rays east to west. Three repetitions are executed for each fruit which are delayed from 3 to 5 days for each repetition. At the end of each day, the samples are wrapped in foil and sealed tightly and stored.

3.1.4 Statistical analysis of the values by treatments

Statistical analysis was contemplated with a complete or random design with therapizations in each of the treatments; the units are practices or experimental comprising of 4 kg of dried fruit. These results are tabulated making use of Statgraphics software and InfoStat™ 5.1TM in terms of linear regression and variance (ANOVA). To identify significant differences in treatments, as well as statistical significance for all comparisons,  $p < 0.05$  was used. The Tukey multirange test was used to compare mean values of treatments.

4. Results

4.1 Bromatological analysis of fruits evaluated

At the bromatology laboratories of the Agricultural Polytechnic School in Manabí Manuel Félix López (ESPAM MFL) and CE.SE. C.CA Unibersidad Laica Eloy Alfaro de Manabí (ULEAM), Manta, Ecuador, analysis of moisture, ash, proteins and fiber is conducted, and 250 g was manipulated for each sample, published in Table 1.

The percentage of humidity in pineapple decreased from 86.36 to 21.14%, in mamey from 79.30 to 21.07%, and banana from 80.22 to 10.35%; ashes amount in pineapple from 0.44 to 1.09%; in mamey from 0.25 to 2.66%, and in bananas from 1.12 to 2.80% indicating that in the latter, it is higher than the previous fruits.

For pineapple protein amounts from 0.67 to 2.45%; for mamey from 0.41 to 2.55%, and for banana from 1.27 to 2.14%; in this case the three fruits increased their amounts, and finally the amount of fiber in pineapple is from 2.05 to 3.63%, in

| Fruit state      | Parameters | Method            | Unity | Pineapple | Mamey | Banana |
|------------------|------------|-------------------|-------|-----------|-------|--------|
| Fresh fruit      | Moisture   | INEN 864          | %     | 86.36     | 79.30 | 80.22  |
|                  | Ash        | INEN 467          | %     | 0.44      | 0.25  | 1.12   |
|                  | protein    | PEE/SECECCA/QC/15 | %     | 0.67      | 0.41  | 1.27   |
|                  | Fiber      | PEE/SECECCA/QC/03 | %     | 2.05      | 2.50  | 0.88   |
| Dehydrated fruit | Moisture   | INEN 864          | %     | 21.14     | 21.07 | 10.35  |
|                  | Ash        | INEN 467          | %     | 1.09      | 2.66  | 2.80   |
|                  | protein    | PEE/SECECCA/QC/15 | %     | 2.45      | 2.55  | 2.14   |
|                  | Fiber      | PEE/SECECCA/QC/03 | %     | 3.63      | 4.94  | 2.42   |

Table 1.  
Bromatological analysis on fresh and dehydrated fruits.



mamey from 2.50 to 4.94%, and in banana from 0.88 to 2.42% of the same way augments, respectively.

4.2 System efficiency in each of the fruits

Figure 4 and Table 2 show the moisture extracted against the emission of the radiation; according to this we manage to determine that the molecular structure of the banana facilitates the extraction more accelerated or rapidly with respect to moisture, thus following the pineapple and mamey in which it can be proven that the equipment is more efficient for banana fruit.

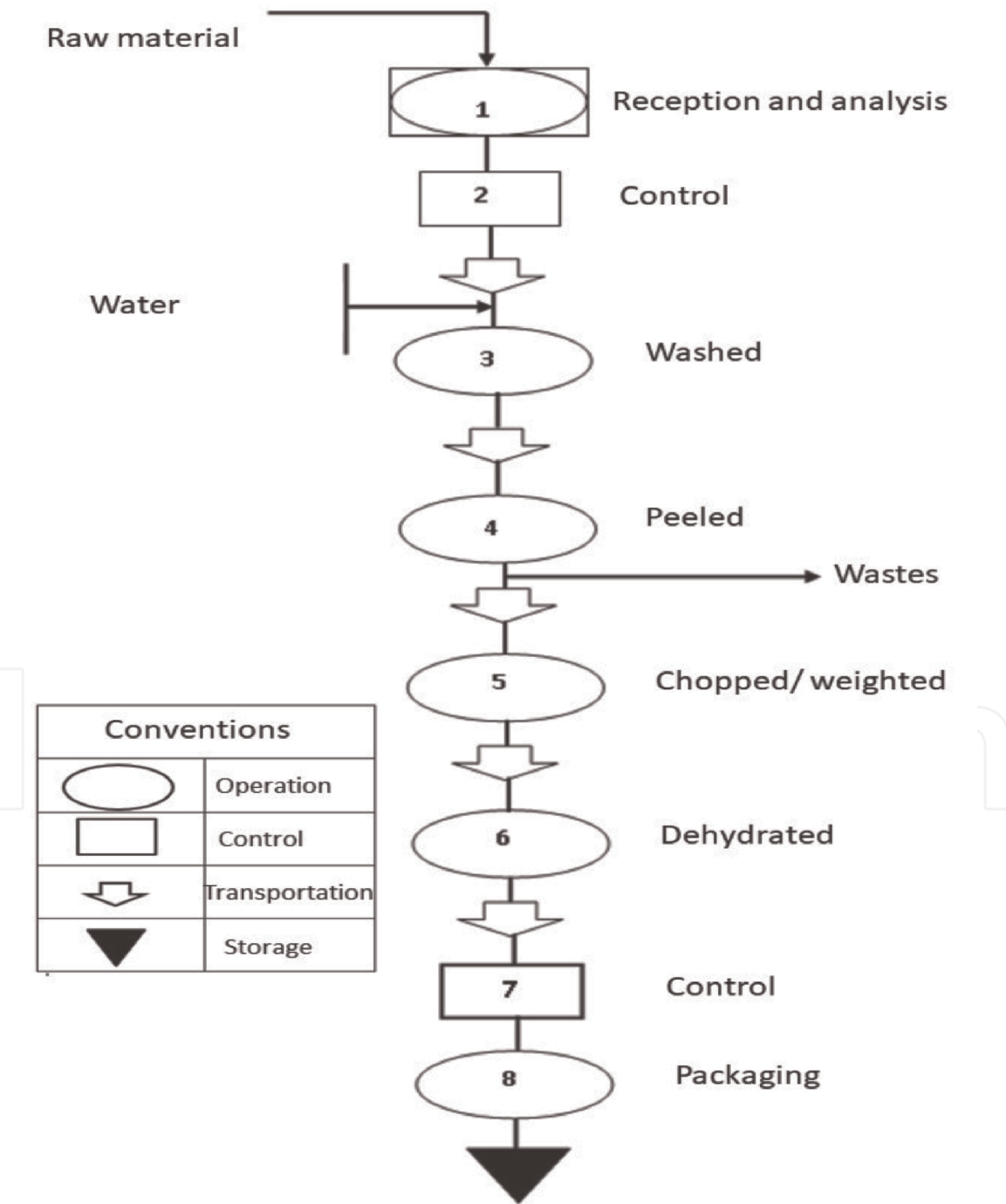
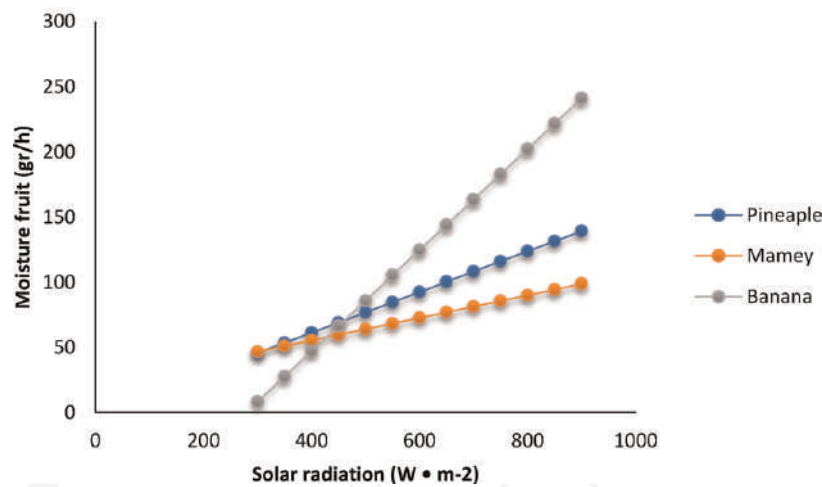


Figure 4.  
Process flow chart of dried pineapple, mamey, and banana fruits.

| Solar radiation (W • m <sup>-2</sup> ) | Pineapple (% H) | Mamey (% H) | Banana (% H) |
|--|-----------------|-------------|--------------|
| 300                                    | 45.61883        | 46.54318    | 8.205        |
| 350                                    | 53.41883        | 50.89206    | 27.606       |
| 400                                    | 61.21883        | 55.24094    | 47.007       |
| 450                                    | 69.01883        | 59.58982    | 66.408       |
| 500                                    | 76.81883        | 63.9387     | 85.809       |
| 550                                    | 84.61883        | 68.28758    | 105.21       |
| 600                                    | 92.41883        | 72.63646    | 124.611      |
| 650                                    | 100.21883       | 76.98534    | 144.012      |
| 700                                    | 108.01883       | 81.33422    | 163.413      |
| 750                                    | 115.81883       | 85.6831     | 182.814      |
| 800                                    | 123.61883       | 90.03198    | 202.215      |
| 850                                    | 131.41883       | 94.38086    | 221.616      |
| 900                                    | 139.21883       | 98.72974    | 241.017      |

**Table 2.**  
*System efficiencies vs. dehydrated fruits.*

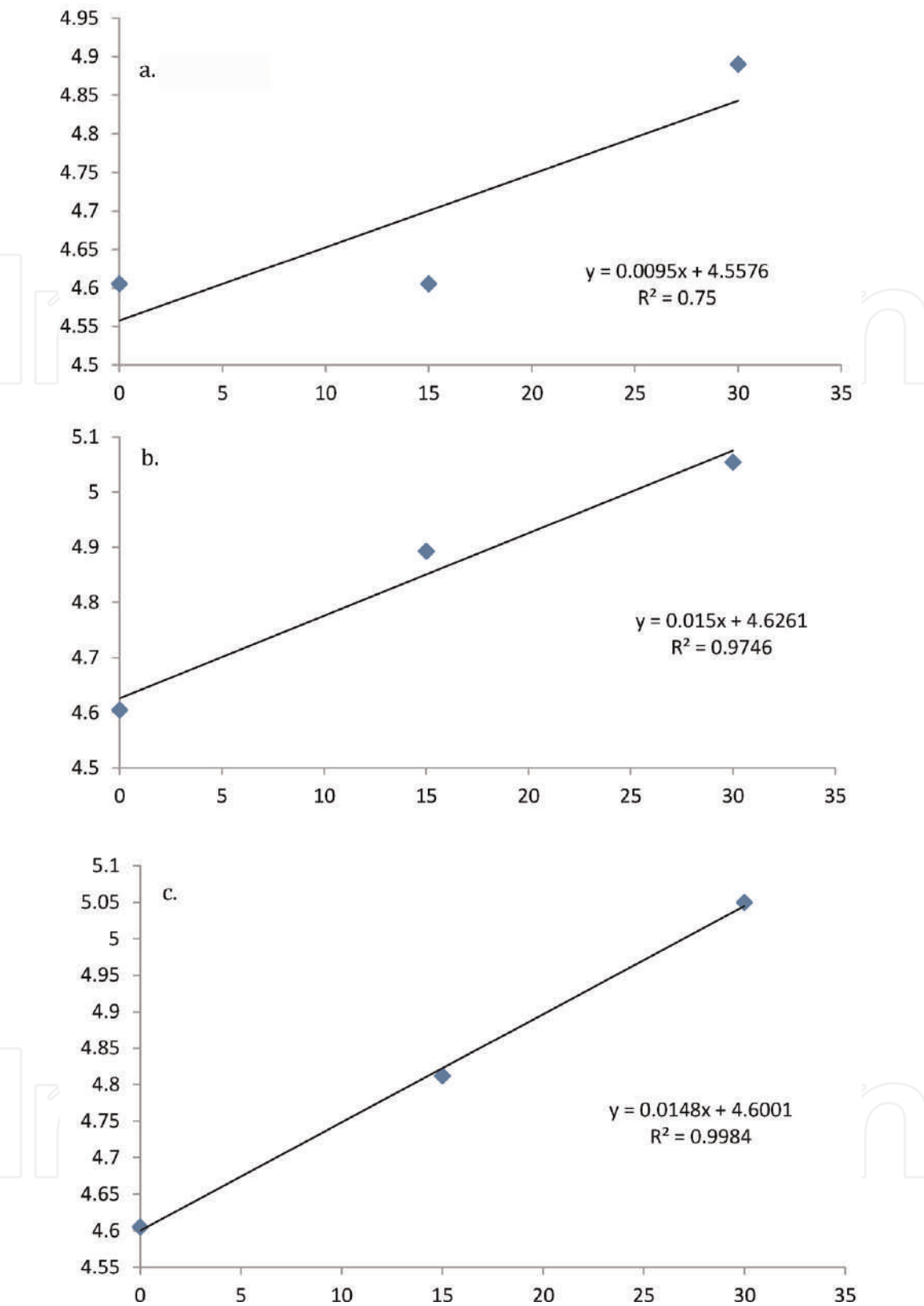


**Figure 5.**  
*Differentiation of water vapor contents as absolute humidity according to solar radiation.*

**Figure 5** shows the moisture variation as a function of solar radiation in the evaluated fruits, pineapple, mamey, and banana, respectively.

### 4.3 Microorganism tests to learn about fruit shelf life

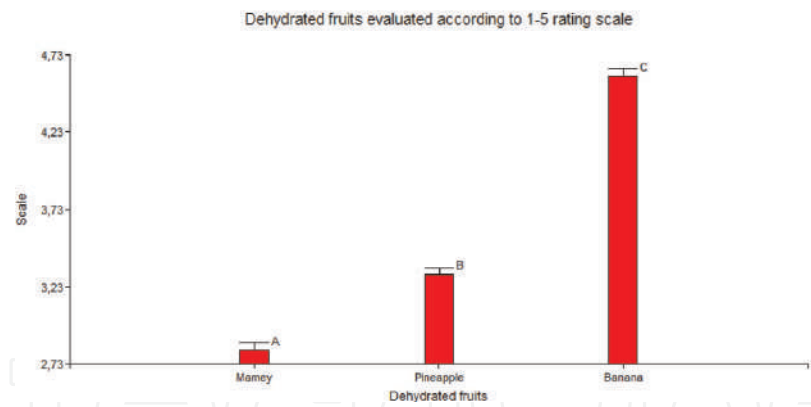
In a given time of 15 and 30 days for the purpose of concerning the fruit drying activities assessed, each repetition is presented with their respective microbiological examinations with units of measurement in CFU.g<sup>-1</sup> which in turn were compared with Ecuadorian Standardization Service (INEN) standards with their details in maximum limits allowed; in other instances the microorganisms found in the samples requested from the microbiology laboratories of the Agricultural Polytechnic School of Manabí Manuel Félix López (ESPAM MFL) are multiplied exponentially, of mathematical type making use of exponents, i.e., the fickle x (unit of measure (d)) suppressed day presents the lifetime data for which the following are assessed: pineapple 174, mamey 106, and banana 109 (**Figure 6**).



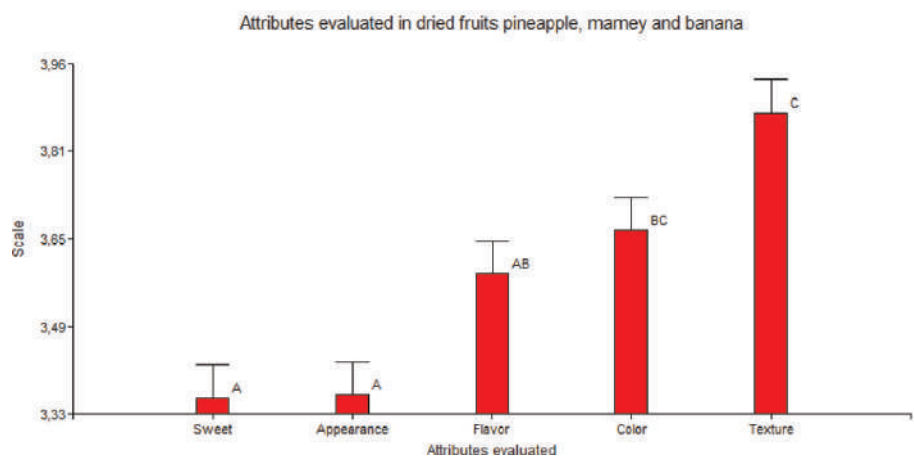
**Figure 6.** Shelf life for dehydrated fruits. (a) Pineapple; (b) mamey; (c) banana.

4.4 Sensory evaluation with scale 1–5

The attributes evaluated were texture, sweetness, aspect, color, and flavor; these were calculated on the basis of the InfoStat software, allowing the most relevant characteristics of the attributes to be in their respective order for dehydrated fruits of pineapple, mamey, and banana, respectively (Figures 7 and 8, Tables 3–5).



**Figure 7.**  
The valuation scale in dehydrated fruits.



**Figure 8.**  
Evaluation of dehydrated fruit acratations depending on the scale score.

| Variable | N   | R <sup>2</sup> | R <sup>2</sup> Aj | CV    |
|----------|-----|----------------|-------------------|-------|
| Scale    | 300 | 0.76           | 0.75              | 12.87 |

**Table 3.**  
Analysis of variance.

| F.V.              | SC     | gl  | CM    | F      | p-value |
|-------------------|--------|-----|-------|--------|---------|
| Model             | 193.09 | 14  | 13.79 | 65.32  | <0.0001 |
| Factor A          | 168.56 | 2   | 84.28 | 399.17 | <0.0001 |
| Factor B          | 11.12  | 4   | 2.78  | 13.16  | <0.0001 |
| Factor A*Factor B | 13.42  | 8   | 1.68  | 7.94   | <0.0001 |
| Error             | 60.17  | 285 | 0.21  |        |         |
| Total             | 253.27 | 299 |       |        |         |

**Table 4.**  
Variance analysis (SC type I).

| error: 0.2111 gl: 285  |            |      |    |      |   |       |
|--|------------|------|----|------|---|-------|
| Factor A   | Factor B   | Half | n  | E.E. |   |       |
| Mamey  | Sweet      | 2.48 | 20 | 0.10 | A |       |
| Mamey  | Appearance | 2.51 | 20 | 0.10 | A |       |
| Mamey  | Flavor     | 2.53 | 20 | 0.10 | A |       |
| Pineapple  | Appearance | 2.91 | 20 | 0.10 | A | B     |
| Pineapple  | Sweet      | 3.03 | 20 | 0.10 |   | B C   |
| Mamey  | Color      | 3.21 | 20 | 0.10 |   | B C D |
| Mamey  | Texture    | 3.35 | 20 | 0.10 |   | B C D |
| Pineapple  | Color      | 3.40 | 20 | 0.10 |   | B C D |
| Pineapple  | Flavor     | 3.48 | 20 | 0.10 |   | C D   |
| Pineapple  | Texture    | 3.70 | 20 | 0.10 |   | D     |
| Banana   | Color      | 4.38 | 20 | 0.10 |   | E     |
| Banana   | Sweet      | 4.58 | 20 | 0.10 |   | E     |
| Banana   | Texture    | 4.58 | 20 | 0.10 |   | E     |
| Banana   | Appearance | 4.68 | 20 | 0.10 |   | E     |
| Banana   | Flavor     | 4.75 | 20 | 0.10 |   | E     |
| Means with a common letter are not significantly different ( $p > 0.05$ ). |            |      |    |      |   |       |

**Table 5.**  
Test: Tukey Alpha = 0.05 DMS = 0.49402.

**4.5 Relationship and recoil tests concerning the access temperature in dryer with the receiver access sheet (collector), as well as the radiation with the low amounts of water as absolute humidity in the fruits of pineapple, mamey, and banana**

Based on p-value in ANOVA calculated less than 0.01, therefore, there is a significant relationship from the statistical level, between the drying T°C and the plate T°C with 99% confidence level.

R<sup>2</sup> indicates the percentage (%) variation of the response variable that explains its relationship to one or more predictor variables; it can be said that the higher the R<sup>2</sup>, the better the arrangement of the model to the obtained data.

So according to this premise, the model exposes 61.3763% variability in drying T°C, and the correlation coefficient is equal to 0.78343; therefore, it indicates a moderately strong relationship between the variables, and the standard error evaluation shows in the calculation that the standard deviation of the residuals is 2.51359.

Regression exam/linear pattern  $Y = a + b * x$ .

Dependent variable (VD): drying T°C

Independent variable (VI): plate T°C

The results expose the output, and it conforms to the linear model to refer to the relationship between the drying T°C with the plate T°C.

The equation of the adjusted model below is

$$Drying\ T^{\circ}C = 20.0773 + 0.275953 * plate\ T^{\circ}C \tag{1}$$



4.5.1 Regression examination between drying temperature and receiver temperature (collector)

Depending on p-value in ANOVA less than 0.01, therefore, there is a significant statistical relationship between the drying T°C and the T°C of the collector with a level of 99% confidence.

R<sup>2</sup> indicates that the model exposes 59.672% variability in drying T°C, and the correlation coefficient is equal to 0.772477, therefore indicating a moderately strong relationship between the variables (**Figure 9**).

Regression exam/linear pattern  $Y = a + b * x$

Dependent variable (VD): drying T°C

Independent variable (VI): collector T°C

The results expose the output, and it conforms to the linear model to refer to the relationship between the drying TOC and the collector TOC.

The equation of the adjusted model below is

$$\text{Drying T}^\circ\text{C} = 23.2088 + 0.269216 * \text{Collector T}^\circ\text{C} \tag{2}$$

4.5.2 Pineapple fruit and your regression exam

Depending on p-value in the ANOVA less than 0.01, there is a significant statistical relationship between DMP and SRP with a 99% level of trust.

R<sup>2</sup> indicates that the model exposes 48.0814% variability in DMP. The correlation coefficient is equal to 0.693408; therefore, it indicates a moderately strong relationship between the variables, and the standard error evaluation of the sample in the calculation shows that the standard deviation of the residuals is 23.4888 (**Figure 9a**).

Linear pattern  $Y = a + b * x$

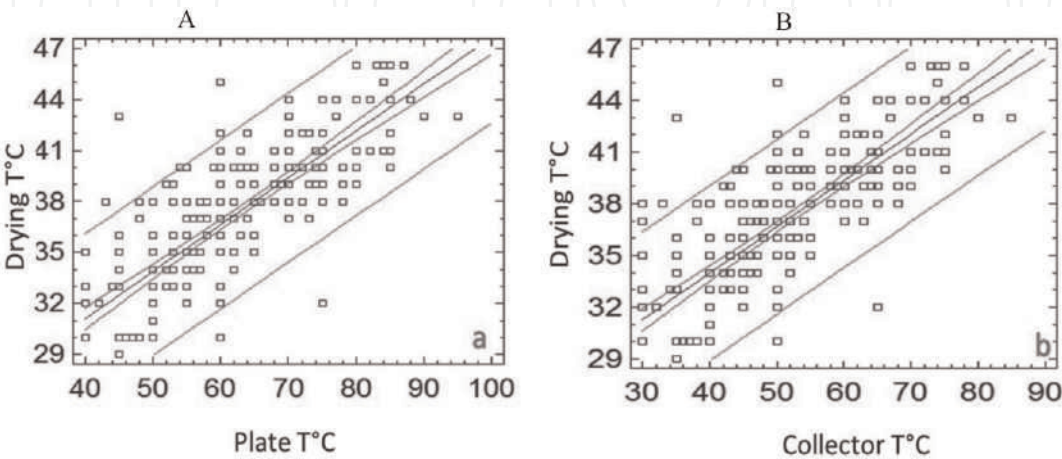
Dependent variable (VD): decreasing moisture pineapple (DMP)

Independent variable (VI): solar radiation pineapple (SRP)

The effects of linear model adjustment refer to the relationship between DMP and SRP.

The equation of the adjusted model below is

$$\text{DMP} = -1.18117 + 0.156 * \text{SRP} \tag{3}$$



**Figure 9.** Drying inlet with plate temperature (a) and receiver temperature (collector) (b), where the adjusted model is displayed.

#### 4.5.3 Mamey fruit and your regression analysis exam

Depending on the p-value in ANOVA calculation which is less than 0.01, there is a significant statistical relationship between DMM and SRM with a confidence level of 99%. The  $R^2$  states according to model that there is 55.6423% variability in DMM, the correlation coefficient is equal to 0.745938; therefore, it shows a moderately dynamic relationship between the variables, and the standard error evaluation shows that the standard deviation of the residuals is 12.3989 (**Figure 9b**), as well as the average absolute error (AAE) of 10.7287.

Linear pattern  $Y = a + b * x$

Dependent variable (VD): decreasing moisture mamey (DMM)

Independent variable (VI): solar radiation mamey (SRM)

The effects of linear pattern adjustment to refer to the dependency between DMM and SRM.

The equation of the adjusted model below is

$$DMM = 20.4499 + 0.0869776 * SRM \quad (4)$$

#### 4.5.4 Banana fruit and your regression analysis exam

Based on ANOVA's p-value in calculation less than 0.01, there is a significant statistical ratio of DMB to SRB with a confidence level of 99%, while  $R^2$  exposes according to model that there is 56.339% variability in DMB; in other instances the correlation coefficient the evaluation is equal to 0.750593; therefore, it teaches the coordinately dynamic relationship between the variables and finally the standard evaluation error presenting a value of 35.5063 (**Figure 10c**). The mean absolute error (AAE) is 24.6024.

Linear pattern  $Y = a + b * x$

Dependent variable (VD): decreasing moisture banana (DMB)

Independent variable (VI): solar radiation banana (SRB)

The effects of linear pattern adjustment refer to the dependency between DMB and SRB.

The equation of the adjusted model below is

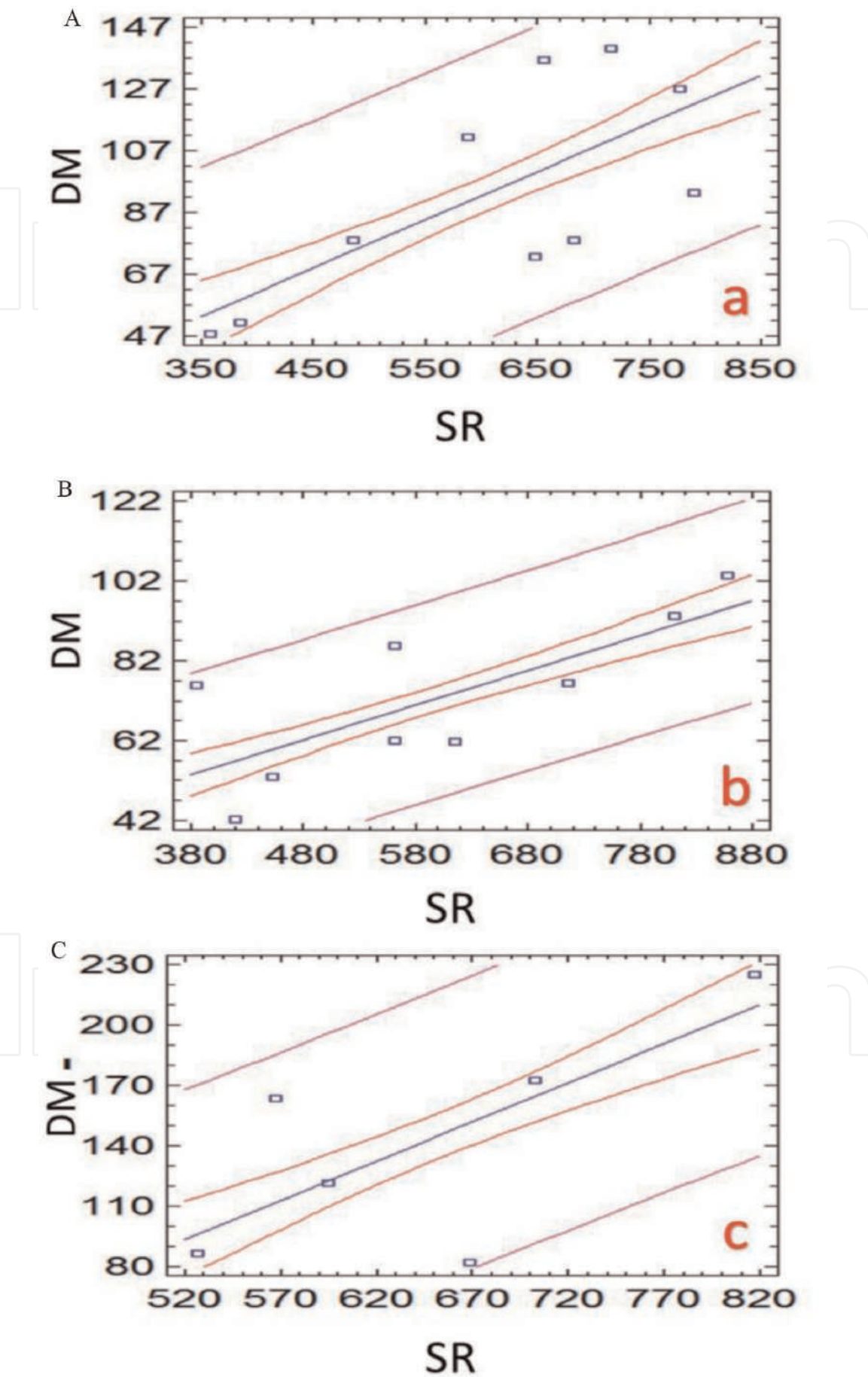
$$DMB = -108.201 + 0.38802 * SRB \quad (5)$$

### 4.6 Examination of the process by psychometric spread

The leaf concerning psychometric dehydration consents to be able to observe two autonomous methodologies, i.e., at one point, there is a sensitive air heated in the receiver or collector, in which air entering the apparatus is heated at the cost of emissions of solar radiation sponsoring moisture content firmly, and consecutively, in other instances the air develops moisture by vaporizing water in the fruits of pineapple, mamey, and banana as a result of cooling. As an example, in the first process of dehydration of banana fruit, we assume subsequent identifications with their means: air temperature, 26°C; first relative humidity, 72%; air temperature at the dryer inlet as well as the leak in the receiver (collector), 49°C; air temperature in dryer escape, 35.7°C; air channel diameter, 0.08 m; speed of air at the entrance, 16.6 m.s<sup>-1</sup>; and separate humidity of water, 172.43 g.

### 4.7 Through these ante-laid characterizations, the movement of the mass fluids was established using the following equations

$$W = \frac{\pi * d^2}{4} * V * p \quad (6)$$



**Figure 10.**  
Pattern provided towards low humidity in fruits dehydrated, (a) pineapple, (b) mamey, and (c) banana, with respect to solar radiation.

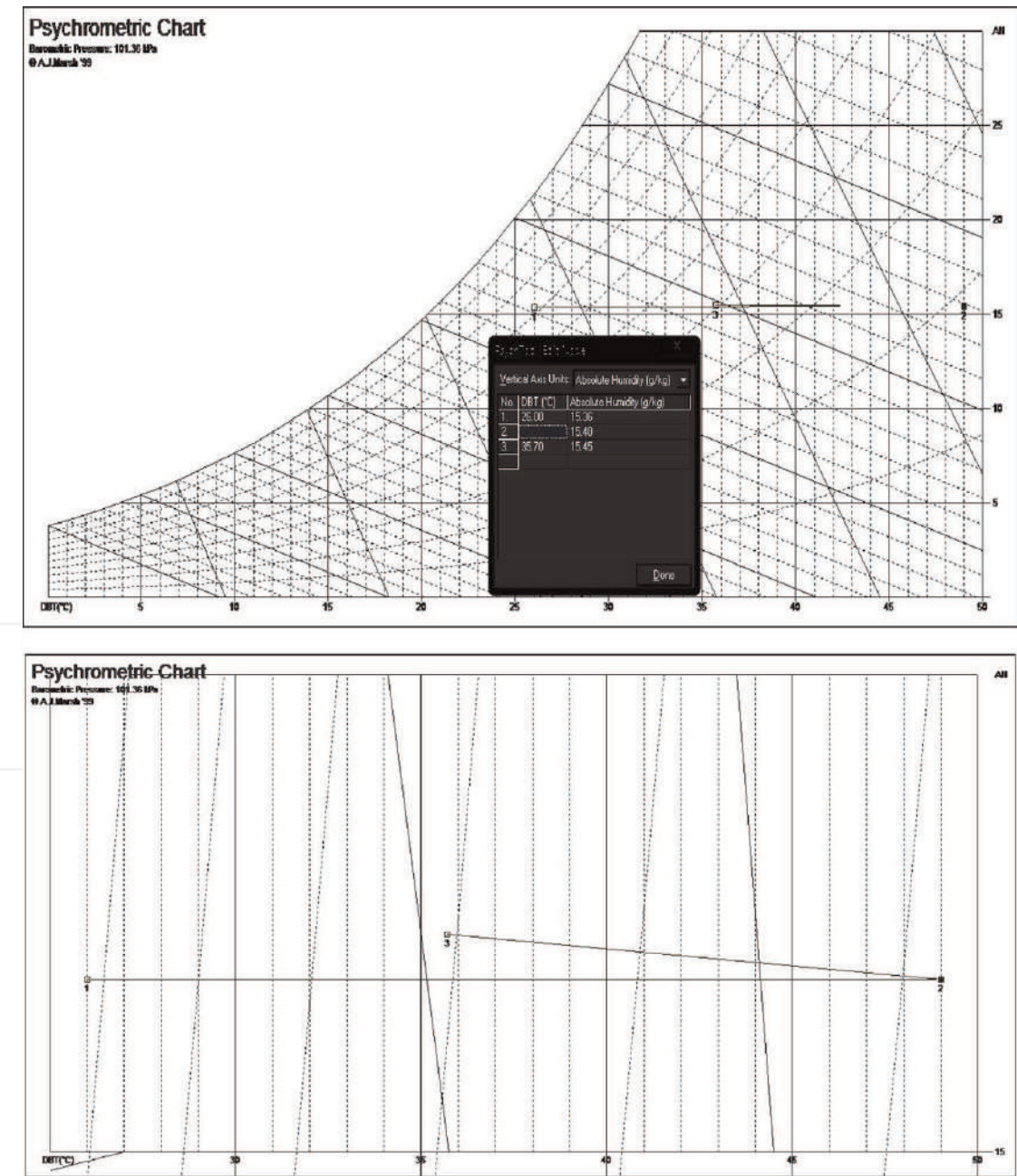


where  $d$  is the diameter of the air channel and  $V$  is the speed of air as well as the air density, resulting in the value of  $0.083 \text{ kg.s}^{-1}$ . Consecutively after these values and identifying the suppressed humidity of the fruits, the portion of water absorbed in kg of air entering the dryer in the staged phase is established by using Eq. (7):

$$d = \frac{172.43 \text{ g water}}{1801 \text{ k dried air}} = 0.095 \frac{\text{g}}{\text{k}} \tag{7}$$

In **Figure 11**, you can observe the thermodynamic moments of sites 1, 2, and 3 provided to the air and habitat, in the receiver leak (collector) as well as in the dryer leak; therefore, these identifications, as data taken from psychrometric chart software, manifest the temperature of the dry lamp(DB); relative humidity (RH); absolute humidity (AH); specific volume (Vol); enthalpy(Ent); steam pressure (VP); dew point(DP); and wet bulb temperature (WBT).

The case in process 1–2 was framed concerning reflective heating in the solar receiver (collector), while in other instances in the case corresponding to process



**Figure 11.**  
*Examination of the table in collector and solar dryer in the form of a psychrometric chart.*

2–3 in the inlet dryer, the humidification of the air and its convenient cooling were carried out through the activities of evaporation of water included in the fruits of pineapple, mamey, and banana.

## 5. Debate

In **Table 1**, we can disclose the percentage (%) of humidity above what was known after the dehydration activities: for pineapple with 86.36%, the moisture content is reduced by an average of X 2.14%, in mamey with 79.30%, by an average of X 21.07%, and for banana with a total of 80.22%, by an average of X 10.35%. The data are consistent with ante positioned knowledge executed by Almada (see [9]). There are also other intellectual citations covered in the mastery of the convective multiflash desiccation process (CMFD) (see [7–11]) are correlated in dried fruits, the inquiry as a study subject, for banana fruit were heated at 60°C by hot air as well as a vacuum pulsation was used, therefore consecutively in the drying of the fruit by medium of the convective drying and dizzying banana vaporization mixture, by CMFD, showed a moisture amount at 0.293 g.g<sup>-1</sup> (dry base) then in 3 h of process, the pattern of heat diagnosed in banana samples existed through the direction (conduction) and solar luminescence, so they were heated by approximately 60°C, large increases in independent or free water (banana moisture content at 76.00%), coinciding with the illustrations executed (see [10, 11]).

Subsequently in the convective multiflash drying process (CMFD) (about 135 min of process), the banana achieved a moisture amount in 0.29–0.01 g.g<sup>-1</sup>; finally in the processing, the quantities were 0.276–0.015. The fruits with average amounts of moisture showed a water action ranging from 0.65, 0.85 to 0.90, while the mass of the fruits, due to dehydration, was noted with reduced amount of water and dominoes up to 60.21 g of solid in each repetition of 500 g of dough, mainly because of the water and native mechanisms are transferred to the osmotic procedure from extracellular areas, producing an ascent in the aroma of the fruit as well as well as the texture (see [11, 12]).

This work resolved to disinfect at 180°C for 60 min according to internationally determined rules such as the Medical Research Council; fruits such as banana amounts in 80.22% moisture in fresh state. Together, the validity of the dehydrator was select, assuming the similarity of the convective multiflash drying process (CMFD) method (see [4]) and the solar dryer. In both cases containing the use of solar radiation emission, these being at 300–900 W•m<sup>-2</sup> (see [13]) the proportion of solar radiation previously and subsequently in the matter of dehydration within the process activities, the banana fruit had a reduction of 80.22–10.35%, exposing that subsequently it is being subjected to 180°C for 60 min a day with a total of 15–30 days. Its index was 0.12% concerning 10.35%, pointing to 0.4 times minimum amount in parallel in banana fruit.

The convective multiflash drying process (CMFD) is a method of efficient dehydration due to two important reasons. Firstly because during flash evaporation, it starts from moisture that encloses internally, so it is pull towards the surface of the fruits, making optimal the convective drying during the movement for heating purposes. Secondly we have to subsequently evaporate the flash, and the fruit is stothered to the surface area of it, making optimal the convective drying during the heating movement as well as later in the evaporation of the flash. The temperature of the fruit drops by 15–20°C, so it transports a relevant difference in the temperature between the hot air and the cooled fruit. We could therefore say that because of this, the fruit receives a better transfer of heat, see [7], a method similar to the procedure or technique assessed in this investigation as the object of study.



Having had on balance, all this provides more accurate and complete assessments of the duration as useful life of dehydrated fruits, in pineapple, mamey and banana individually, of 15–30 days of dehydration process in repetitions, the amount of the shelf life of banana fruit, by sample, see **Figure 5**, as linear regressions with adjusted model of the low humidity of banana fruit in this regard with radiation showed a duration of 109 days, the moisture content of pineapple was reduced from the amount or average riginaria by 86.36% to a final amount of 21.07%; mamey fluctuated between 79.3 and 21.13% and bananas fluctuated between 80.22 and 10.35%, proportionally. As well as, properties such as ash in pineapple at 0.44% had an increase with an average of 1.09%; 0.25% had an increase of 2.66%, and in banana fruit it fluctuated between 1.12 and 2.80%, exposing, in banana farmed fruits, data with more expensive values (data not exposed).

The protein content, as well as fiber, was known a characteristic increase significantly in the previous and subsequent periods in dehydration, is understood as a derivation of fresh pineapple fruit in 0.67% protein and fibers at 2.45% in its fresh phase, together, in dehydrated period, had an increase of 2.45 and 3.63%. The mamey fruit with 0.41% protein and fiber sin at 2.5% in its fresh period, in its dehydrated period, had an increase of 2.55 and 4.94%, proportionally, finally, in banana fruit with amounts of protein type by 1.27 and 0.88% in its fresh, dehydrated time, had an increase of 2.18 and 2.41%, correspondingly.

## 6. Termination

This work as an object of study in the research assessed the incidences of a solar dryer, which in turn was developed in the city of Calceta, in Bolívar Canton of the Province of Manabí, Ecuador, with the approach of drying to such a point of being able to talk about the phenomena concerning the dehydration of fruits such as pineapple, mamey, and banana. Therefore, trials were carried out as experiments finding, for example, that the organization of the molecular structure of the banana provides the facility for moisture content by means of solar radiation activity.

Then, followed by the pineapple fruit and mamey, as a result, this loss is compressing the moisture content of the valued fruits. The temperature of the drying air is the most important and effective component of several elements of the system during drying; air humidity, as well as air speed, is also a significant factor in optimizing the drying rate. Therefore, in these concerns, it is understood that the microbiological examination helps to establish the shelf life of dehydrated fruits, and it is more important to mention that from 15 to 30 days, repetitions in measured quantities CFU.g<sup>-1</sup> have given legitimate maximum values, which is understood as a result of the proliferation of microorganisms in the fruits evaluated.

## Acknowledgements

We thank the Unibersidad Laica Eloy Alfaro de Manabi (ULEAM), Ecuador, for being part of the university community as teachers and researchers, Secretariat of Higher Education, Science, Technology and Innovation (Senescyt), and Faculty of Agricultural Sciences of the Agroindustrial Engineering Career in turn that in some way or another allows us to universalize knowledge and transmit it to students.

## Dedication

This chapter of the book is dedicated to God, who gives me day-to-day forality to make the daily activities, to my wife Emily Julissa Mendoza Cedeño and daughter

Hadassah Julissa Bello Mendoza for their spiritual support and words of encouragement to make diary, and to my esteemed fraternal friend Edgar Ruperto Macías Ganchozo whose idea and professional work could have made this chapter a reality for his knowledge.

Appendices and nomenclature

Roman symbols

|                |  |
|----------------|--|
| E              | solar radiation intensity ( $W \cdot m^{-2}$ ) |
| A              | surface area ( $m^2$ )                         |
| n              | number of experiments                          |
| CFU            | colony-forming unit                            |
| t              | temperature                                    |
| h              | specific enthalpy (kJ/kg)                      |
| RH             | relative humidity                              |
| AH             | absolute humidity                              |
| Vol            | specific volume                                |
| VP             | vapor pressure                                 |
| DP             | dew point                                      |
| WBT            | temperature of wet bulb                        |
| R <sup>2</sup> | percentage of variation of the variable        |
| Eq.            | equation                                       |
| AAE            | average absolute error                         |

Greek symbols

|        |           |
|--------|-----------|
| $\tau$ | time, min |
|--------|-----------|

Subscripts

|      |   |
|------|---|
| amb  | ambient (at 25°C, 30 wt % relative humidity, 1.012 bar) (kJ/kg) |
| DM   | dry matter  |
| CMFD | convective multflash drying process                             |
| W    | water   |
| D    | the drying chamber of the drying process                        |
| DMP  | decreasing moisture pineapple                                   |
| SRP  | solar radiation pineapple                                       |
| DMB  | decreasing moisture banana                                      |
| SRB  | solar radiation banana  |
| DMM  | decreasing moisture mamey                                       |
| SRM  | solar radiation mamey   |

IntechOpen

### Author details

Italo Pedro Bello Moreira\*, Edgar Ruperto Macías Ganchozo,  
Xavier Enrique Anchundia Muentes, Celio Danilo Bravo Moreira,  
Manuel Eduardo Anchundia Muentes, Hebert Edison Vera Delgado  
and Carlos Eduardo Anchundia Betancourt

Faculty of Agricultural Sciences, Career of Agroindustrial, Agricultural  
and Environmental Engineering of the Laica University “Eloy Alfaro” of Manabi,  
Manta, Ecuador

\*Address all correspondence to: [italop.bello@uleam.edu.ec](mailto:italop.bello@uleam.edu.ec)

### IntechOpen

© 2020 The Author(s). Licensee IntechOpen. This chapter is distributed under the terms of the Creative Commons Attribution License (<http://creativecommons.org/licenses/by/3.0>), which permits unrestricted use, distribution, and reproduction in any medium, provided the original work is properly cited. 

## References

- [1] Hernández RJ, Flores MF, Acosta OR, Barbosa PG. Secado solar de productos agrícolas. *Caos Conciencia*. 2014;**8**(1): 25-34. Available from: [http://dci.uqroo.mx/RevistaCaos/2014\\_vol1/Secado\\_Solar.pdf](http://dci.uqroo.mx/RevistaCaos/2014_vol1/Secado_Solar.pdf)
- [2] Hernández RJ, Martínez VO, Quinto DP, Cuevas DJ, Acosta OR, Aguilar JO. Secado de chile habanero con energía solar. *Revista Iberoamericana de Tecnología Postcosecha*. 2010;**10**(2):120-127. Available from: <http://www.redalyc.org/articulo.oa?id=81315091008>
- [3] Reinoso B, Diseño ES. Construcción de un secador experimental de hierbas aromáticas con el empleo de energía solar, Capacidad de 5 Kg [Thesis]. Sangolquí/ESPE, Ecuador: Universidad de Fuerzas Armadas; 2006
- [4] Zotarelli M, Almeida PB, Borges LJ. A convective multi-flash drying process for producing dehydrated crispy fruits. *Journal of Food Engineering*. 2011; **108**(4):523-531. DOI: 10.1016/j.jfoodeng.2011.09.014
- [5] García AI, Justinovich S, Angel L, Heredia T. Secadero solar forzado para productos agrícolas. *Averma*. 2015; **19**(2):21-28. Available from: <http://www.asades.org.ar/Averma/Secadero%20solar%20forzado%20para%20productos%20agricolas>
- [6] Ochoa MCI. Red neuronal artificial en respuesta a predicciones de parámetros de transferencia de masa (pérdida de humedad y ganancia de sólidos) durante la deshidratación osmótica de frutas. *Acta Agronomica*. 2016;**65**(4):318-325. DOI: 10.15446/acag.v65n4.50382
- [7] Azouma YO, Drigalski L, Jegla ZK, Reppich M, Turek V, Weiß M. Indirect convective solar drying process of pineapples as part of circular economy strategy. *Energies*. 2019;**12**(15):2841. DOI: 10.3390/en12152841
- [8] INAMHI-Instituto Nacional de Meteorología e Hidrología de Ecuador. Geoinformación Hidrometeorológica de Manabí y Esmeraldas, Ecuador. Red de Estaciones Meteorológicas Convencionales. Geoinformación Hidrometeorológica de Manabí y Esmeraldas, [Internet]. 2016. Available from: <http://www.serviciometeorologico.gob.ec> [Accessed: 11 September 2019]
- [9] UNESCO. Organización de la Naciones Unidas para la Educación, la Ciencias y la Cultura Guia de Uso, de Secadores Solares para frutas, Legumbres, Hortalizas, Plantas Medicinales y Carnes, Agencia Suiza para el Desarrollo y la Cooperación (Ministerio Suizo de Asuntos Exteriores) [Internet]; Paraguay, Asuncion; 2005. pp. 25-28. Available from: <https://unesdoc.unesco.org/ark:/48223/pf0000156206>
- [10] Sivipaucar C, Curo H, Huancahuari E, Llantoy V, Valderrama A. Cálculo y Construcción de un Secador Solar por Convección Natural para el Secado de Plantas Medicinales no Tradicionales. Huarochirí, Peru: Cedit-Centro de Desarrollo e Investigación en Termofluidos; 2008. pp. 18-30. Available from: [http://sisbib.unmsm.edu.pe/BibVirtual/Publicaciones/rev\\_cedit/2008\\_V03/pdf/a03v3.pdf](http://sisbib.unmsm.edu.pe/BibVirtual/Publicaciones/rev_cedit/2008_V03/pdf/a03v3.pdf)
- [11] Gamboa D, Ibáñez D, Meléndez M, Paredes E, Siche R. Secado de lúcum (Pouteria obovata) empleando la técnica de Ventana Refractante<sup>TM</sup>. *Scientia Agropecuaria*. 2014;**5**(2):103-108. Available from: <http://revistas.unitru.edu.pe/index.php/scientiaagrop/article/view/580/542>

[12] Ortiz GS, Sánchez LL, Valdés RMP, Baena GD, Vallejo CFA. Efecto de la osmodeshidratación y secado en la retención de carotenos en fruto de zapallo. *Acta Agronomica*. 2008;57(4): 269-274. Available from: [https://revistas.unal.edu.co/index.php/acta\\_agronomica/article/view/9265/9923](https://revistas.unal.edu.co/index.php/acta_agronomica/article/view/9265/9923)

[13] CONELEC-Consejo Nacional de Electricidad. In: Tacuri FI, CIE Corporación para la Investigación Energética, editors. *Atlas Solar del Ecuador con fines de Generación Eléctrica* [Internet]. Quito, Ecuador; 2008. Available from: <http://biblioteca.olade.org/opac-tmpl/Documentos/cg00041.pdf>



# We are IntechOpen, the world's leading publisher of Open Access books Built by scientists, for scientists

6,300

Open access books available

171,000

International authors and editors

190M

Downloads

Our authors are among the

154

Countries delivered to

TOP 1%

most cited scientists

12.2%

Contributors from top 500 universities



WEB OF SCIENCE™

Selection of our books indexed in the Book Citation Index  
in Web of Science™ Core Collection (BKCI)

Interested in publishing with us?  
Contact [book.department@intechopen.com](mailto:book.department@intechopen.com)

Numbers displayed above are based on latest data collected.  
For more information visit [www.intechopen.com](http://www.intechopen.com)



# Convective Drying in the Multistage Shelf Dryers: Theoretical Bases and Practical Implementation

*Artem Artyukhov, Nadiia Artyukhova, Ruslan Ostroha, Mykola Yukhymenko, Jozef Bocko and Jan Krmela*

## Abstract

The main advantages regarding the convective drying of the granular materials in the multistage dryers with sloping perforated shelves were represented. Peculiarities of the shelf dryers' hydrodynamics were shown in the research. Various hydrodynamic weighing modes were experimentally justified, and the relevant criteria equations were obtained. The results of investigations regarding the interphase heat and mass transfer were given; criteria dependencies, which predict heat and mass transfer coefficients in the shelf dryers, were proposed. A method to assess the efficiency of the dehydration process at the separate stages of the device and in the dryer, in general, was proposed. The algorithm to define the residence time of the granular material on the perforated shelf with a description of the author's software product for optimization calculation was shown. The shelf dryers' engineering calculation method was presented in this work. The original constructions of devices with various ways to control the residence time of the granular material that stays in their workspace were described. The testing results of the shelf dryer to dry granular materials, such as coarse- and fine-crystalline potassium chloride, sodium pyrosulfate, and iron and nickel powders, were demonstrated.

**Keywords:** convective drying, multistage shelf dryer, hydrodynamics, interphase heat and mass transfer, efficiency of dehydration, engineering calculation, industrial implementation

## 1. Introduction

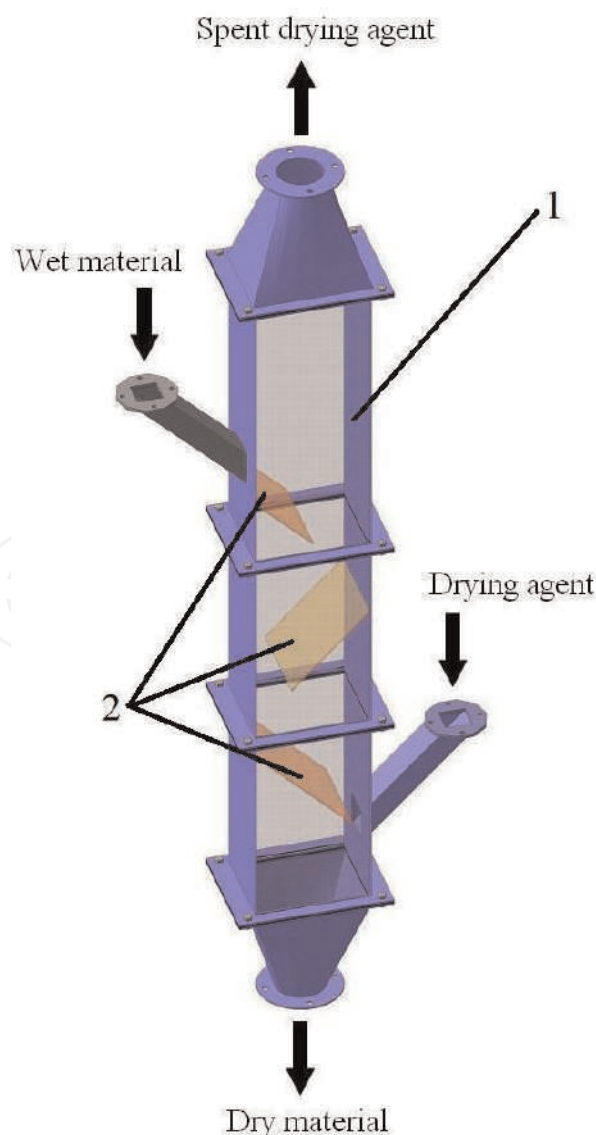
Convective drying is one of the most effective methods for disperse material dehydration in the chemical, pharmaceutical, mining, and other industrial branches [1–6]. The direct contact of the drying agent with high-temperature potential and dried material enables intensively to remove the surface and adsorption-bound moisture [3]. That is why drying is the only method for industries to achieve the required quality of the product.

Although during drying the energy consumption is the lowest, the convective dryers are more often used to dry disperse materials thanks to other numerous

advantages [3, 4]. Provision of the active hydrodynamic regime in such dryers helps intensify the process without reduction of the economic efficiency of their operation and has the following advantages [7–9]:

- Hydrodynamic stability of the process
- Increase of the relative motion velocity of the interacting phases
- The developed surface of the contacting phases
- Approximation of the hydrodynamic model of flows in the device to the ideal displacement model
- Reduction of the energy intensity of the process and metal intensity of devices

One should distinguish devices with various configurations of the weighted layer (fluidized bed, spouting, gravitational falling, vortex, etc.) from the variety of the convective dryer constructions (described, e.g., in [7, 10]). Thanks to the developed surface of the phase contact, devices with hydrodynamic system are characterized with high intensity of the heat and mass transfer processes, lower non-energy costs, and have high specific productivity [7].



**Figure 1.**  
Multistage shelf dryer: (1) case; (2) shelf.

Besides, under conditions of the cost increase to prepare and to transport the drying agent, the possibility of its repeated use in the drying process is fundamentally important. Therefore it is necessary maximum to use the thermal potential of the drying agent during every contact with disperse material. It can be achieved while using the multistage drying devices with vertical sectioning of the workspace by the perforated shelf elements [7, 8, 11].

A solution to the permanent residence of the dispersed material in the “active” zone can be found through implementation of the multistage shelf dryers with vertical sectioning of the workspace (**Figure 1**).

In such devices, the conditions for the differentiated heat treatment of materials can be created owing to the drying agent potential and peculiarities of each stage (shelf) construction. So, moving the perforated shelf to the wall of the device, we approach to the device with fluidized bed, and moving it away from the wall and freeing its workspace, we approach to the device with the free intersection, such as pneumatic transportation dryers. The shelves increase the residence time of the dried material particles, either poured downward of the device or carried out upward of it. The shelves increase the velocity and turbulence of the gas flow, create a vortex motion in their location places, and increase the contact intensity between phases. The free space between the ends of the shelves and the walls of the device does not require special flows from the upper shelf to the lower one. Changing the free area of the shelf perforation, their tilt angles, the distance from the end of the shelves to the walls of the device, the number of shelves, and the distance between them vertically, it is possible to influence the intensity of the contact phases and to create different hydrodynamic regimes to weigh particles of the material both on individual shelves and heightwise the device. Therefore, it is possible to carry out the drying process of wet materials and its pneumatic classification in one device in order to remove small dusty fractions from the mixture [7].

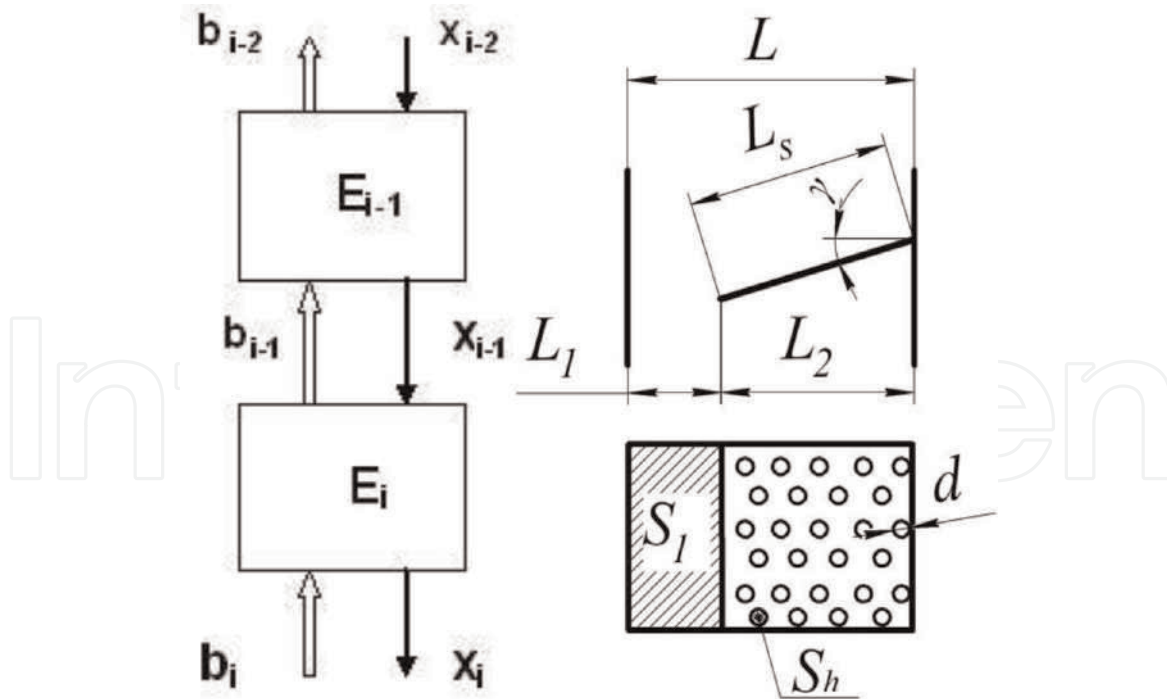
## 2. Theoretical basics

The necessity to determine these features is due to the fact that before constructing an industrial sample of the gravitational shelf dryer it is necessary to determine its optimal design. In this case, the optimization criterion is to ensure the minimum required residence time of the dispersed phase in the working space of the dryer, which will complete the drying process to a predetermined humidity indicator. It is important to observe the condition, under which the “hydrodynamic” residence time of the dispersed phase in the workspace of the device should be no less than the “thermodynamic” time (this parameter is determined by the kinetics of the moisture removal process from the dispersed phase). Therefore, in order to keep the integrity of the dispersed particles, the “hydrodynamic” time should not exceed the “thermodynamic” time by more than 5–10%. By adjusting the hydrodynamic properties of the flow, an optimal construction of the gravitational shelf dryer is achieved, which meets the requirements of the optimization criterion.

Thus, the optimization calculation of the dryer consists of three blocks: hydrodynamic calculation (calculation of the residence time of a particle on a stage), kinetic calculation (kinetic parameter of the moisture removal), and calculation of drying efficiency.

Initial data (**Figure 2**):

- Rate of gas flow,  $Q$  ( $\text{m}^3/\text{s}$ )
- Length of device,  $L$  (m)



**Figure 2.**

*A fragment of the calculation scheme for the multistage drying: left figure—change of flows' moisture:  $x$ , moisture of the disperse material;  $b$ , moisture of the drying agent, and right figure—construction of dryer's workspace.*

- Overall width of device,  $h$  (m)
- Length of shelf,  $L_s$  (m)
- Degree of perforation (free area),  $\delta$
- Perforation hole diameter,  $d$  (m)
- The tilt angle of shelf,  $\gamma$  ( $^\circ$ )
- The radius of the granule,  $r_{gr}$  (m)
- Granule density,  $\rho_{gr}$  (kg/m<sup>3</sup>)
- Gas density,  $\rho_g$  (kg/m<sup>3</sup>)
- Acceleration of gravity,  $g$  (m/s<sup>2</sup>)
- Resistance coefficient,  $\xi$
- Volumetric content of a dispersed phase in a two-phase flow,  $\psi$
- The coefficient that takes into account the tightness of the flow,  $m$
- Number of stages in dryer,  $i$
- Moisture of the material  $i$ -stage of the dryer  $x$  (kg of water/kg of material)
- Moisture of the drying agent in  $i$ -stage of the dryer  $b$  (kg of water/kg of material)



## 2.1 Hydrodynamic calculation

Hole area on the shelf (horizontal position) (m<sup>2</sup>)

$$S_h = \frac{\pi d^2}{4}. \quad (1)$$

The perforated area on the shelf (horizontal position of the shelf) (m<sup>2</sup>)

$$\sum S_h = L_s \cdot h \cdot \delta. \quad (2)$$

Number of holes on the shelf

$$n = \frac{\sum S_h}{S_h}. \quad (3)$$

Area of outloading clearance (m<sup>2</sup>)

$$S_1 = (L - L_s \cos \gamma) \cdot h. \quad (4)$$

Area of the gas passage holes in the shelf (inclined position of the shelf) (m<sup>2</sup>)

$$S_2 = \frac{\pi d^2}{4} \cdot n \cdot \cos \gamma. \quad (5)$$

The relative area of outloading clearance

$$S_1^r = \frac{S_1}{S_1 + S_2}. \quad (6)$$

The relative area of the gas passage holes in the shelf

$$S_2^r = \frac{S_2}{S_1 + S_2}. \quad (7)$$

Rate of the gas flow in outloading clearance (m<sup>3</sup>/s)

$$Q_1 = Q \cdot S_1^r. \quad (8)$$

Rate of the gas flow in holes in the shelf (m<sup>3</sup>/s)

$$Q_2 = Q \cdot S_2^r. \quad (9)$$

Gas velocity in holes in the shelf (m/s)

$$V_{work} = Q_2 / S_2. \quad (10)$$

Second critical velocity (m/s)

$$V_{cr} = 1.63 \cdot \sqrt{\frac{\rho_{dr} \cdot g \cdot r_{gr}}{\xi \cdot \rho_g}}. \quad (11)$$

Velocity difference (m/s)

$$\Delta V = V_{cr} - V_{work}. \quad (12)$$

Time of material residence on the shelf (free movement) (s)

$$\tau_f = \frac{L_s}{\Delta V \sin \gamma} \cdot \tag{13}$$

The empirical function of the effect of compression on the residence time of the particle in the working space of the device

$$f_{e\tau}(\psi) = (1 - \psi)^{-m} \cdot \tag{14}$$

Time of material residence on the shelf (straitened movement) (s)

$$\tau_s = \frac{L_s \cdot f_{e\tau}(\psi)}{\Delta V \sin \gamma} \cdot \tag{15}$$

The program Multistage Fluidizer® [12] used Hypertext Markup Language HTML, Cascading Style Sheet (CSS), and programing language JavaScript (including the library jQuery). HTML is presented as a tagging of web-based app, CSS page formatting. JavaScript is used to calculate and transfer data and to create animation and data validation effect. In the validation block of JavaScript, data accuracy is checked. In the block input info, the basic data field indices are accepted, and they are written to the object of input\_information. In the block, calculation computations are carried out by Eqs. (1)–(15).

Index.html (Figure 3) is the main page of the web-based app. It is responsible for reflection of the main menu, for the main calculation of gas flow, and for jumping the other pages (an example of such page is presented in Figure 4), where the main dependencies between key features to calculate gas flow and resistance time of the material on the shelf are calculated and dependencies diagrams are formed.

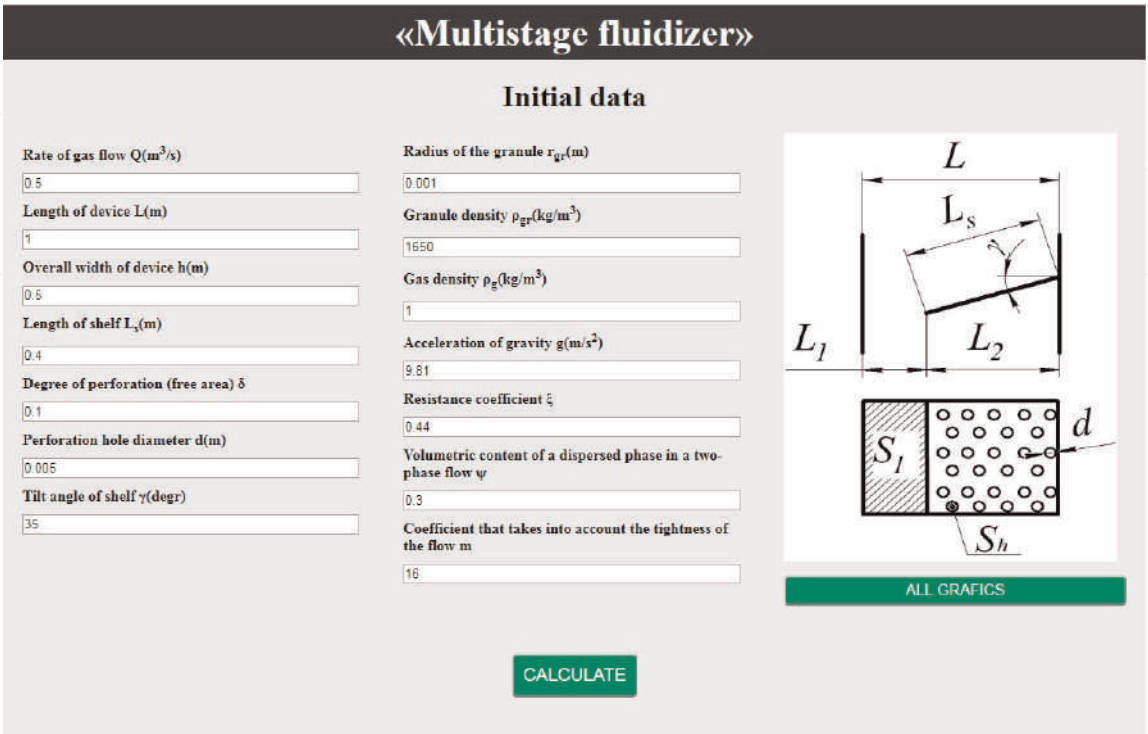


Figure 3.  
The main page of the Multistage Fluidizer® software.

### Influence of radius of the granule on the residence time of a particle

|   |       |
|---|-------|
| Rate of gas flow $Q(\text{m}^3/\text{s})$               | 1     |
| Length of device $L(\text{m})$                          | 0.8   |
| Length of shelf $L_s(\text{m})$                         | 0.7   |
| Overall width of device $h(\text{m})$                   | 1     |
| Minimum radius of the granule $r_{grMin}(\text{m})$     | 0.005 |
| Maximum radius of the granule $r_{grMax}(\text{m})$     | 0.05  |
| Step of radius of the granule $\Delta r_{gr}(\text{m})$ | 0.005 |
| Degree of perforation (free area) $\delta$              | 0.1   |

|  |       |
|--|-------|
| Perforation hole diameter $d(\text{m})$                            | 0.007 |
| Tilt angle of shelf $\gamma(\text{degr})$                          | 15    |
| Granule density $\rho_{gr}(\text{kg}/\text{m}^3)$                  | 1650  |
| Gas density $\rho_g(\text{kg}/\text{m}^3)$                         | 1     |
| Acceleration of gravity $g(\text{m}/\text{s}^2)$                   | 9.81  |
| Resistance coefficient $\xi$                                       | 0.44  |
| Volumetric content of a dispersed phase in a two-phase flow $\psi$ | 0.3   |
| Coefficient that takes into account the tightness of the flow $m$  | 16    |

CALCULATE

Figure 4.  
Calculation page of various parameter impacts on the particle resistance time in the device.

Having inserted data, data validity is tested, that is, if all data is correct, after keystroke CALCULATE data is processed given the above formulas, and we receive the result in a form of a computation table (Figure 5).

After changes of indices  $l_f$  and  $l_s$ , it is possible to see how the animation appears after the pressing the “Show calculation” button (the example of distance length calculation, which particle takes on the shelf during the specified period of time, is shown in Figure 6). In order to create animation, functions clicker\_lf and clicker\_ls are implemented, respectively, for  $\tau_f$  and  $\tau_s$  animation.

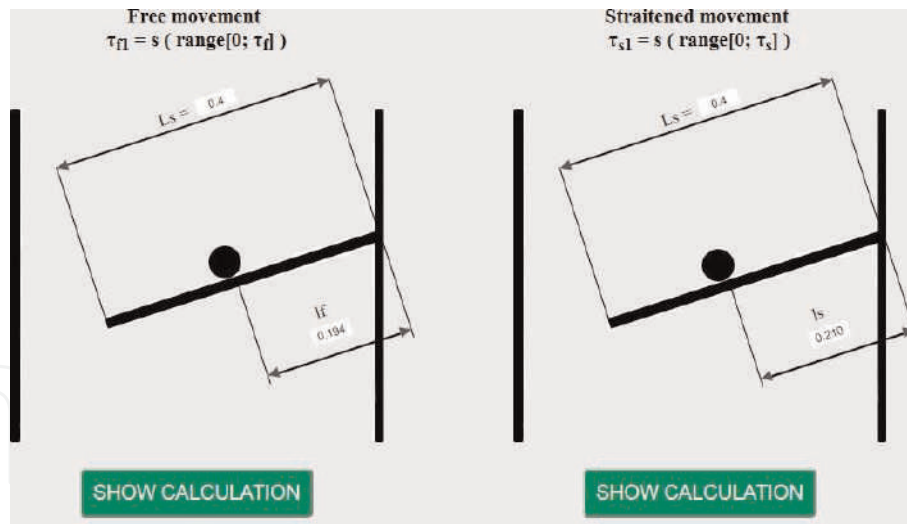
In JavaScript, one uses libraries jQuery and table2excel, objects for data recording, methods .val() .append() to read and to insert indices to fields, methods

### Calculation of the residence time of a particle on a stage

|  |            |
|--|------------|
| Hole area on the shelf (horizontal position), $S_h(\text{m}^2)$                            | 0.00001963 |
| Perforated area on the shelf (horizontal position of shelf), $\Sigma S_h(\text{m}^2)$      | 0.02000    |
| Number of holes on the shelf $n$   | 1019       |
| Area of outloading clearance, $S_1(\text{m}^2)$  | 0.3362     |
| Area of the gas passage holes in the shelf (inclined position of shelf), $S_2(\text{m}^2)$ | 0.01638    |
| Relative area of outloading clearance $S_1^r$  | 0.9535     |
| Relative area of the gas passage holes in the shelf $S_2^r$                                | 0.04647    |
| Rate of gas flow in outloading clearance, $Q_1(\text{m}^3/\text{s})$                       | 0.4768     |

|   |         |
|---|---------|
| Rate of gas flow in holes in the shelf, $Q_2^r(\text{m}^3/\text{s})$  | 0.02323 |
| Gas velocity in holes in the shelf, $V_{work}(\text{m}/\text{s})$   | 1.418   |
| Second critical velocity, $V_{cr}(\text{m}/\text{s})$   | 9.886   |
| Velocity difference, $\Delta V(\text{m}/\text{s})$  | 8.468   |
| Time of material residence on the shelf (free movement), $\tau_f(\text{s})$   | 0.08235 |
| Empirical function of the effect of compression on the residence time of the particle in the working space of the device $f_{et}(\psi)$ | 300.9   |
| Time of material residence on the shelf (strained movement), $\tau_s(\text{s})$   | 24.78   |

Figure 5.  
Results of calculation.



**Figure 6.**

Calculation of way length, which particle undergoes on the shelf during the specified period of time.

.removeClass() and .addClass() to delete and to add classes, and method .animate() for work with animation to create an animation effect for any digital CSS feature of the element.

## 2.2 Calculation of heat-mass transfer

In order to calculate the kinetic parameter of the moisture removal (the moisture-yielding capacity coefficient), let us use the following algorithm.

It is proposed [8] to use the following equation for calculation of  $\beta$ :

$$\frac{\Delta U_m}{\tau} = \beta \cdot F \cdot \left( b_{fin} - \frac{b_{fin} + b_{in}}{2} \right) \cdot \rho_g, \quad (16)$$

where  $b_{in}$ ,  $b_{fin}$ , and  $\Delta U_m$  are the initial and final humidity of the drying agent and the amount of the removed moisture from the material;  $F$  is the surface of the mass transfer, which depends on the dryer's effective operation due to the disperse material and the residence time of the material in the dryer.

In general, the criteria equation of the drying process can be written as follows:

$$Sh = A_1 \cdot Sc^n \cdot Re^m, \quad (17)$$

where  $A_1$  is the equation coefficient;  $Sh = \frac{\beta \cdot d_{gre}}{D}$  is the Sherwood criterion;  $d_{gre}$  is the equivalent diameter of the particle (granule),  $m$ ;  $Sc = \frac{\nu}{D}$  is the Schmidt criterion;  $Re = \frac{V_{work} \cdot d_{gre}}{\nu}$  is the Reynolds criterion;  $D$  is the diffusion coefficient of the gas flow,  $m^2/s$ ;  $\nu$  is the kinematic viscosity coefficient of the gas flow,  $m^2/s$ ; and  $m$  and  $n$  are the indicators of the equation stages, which are evaluated through the graphical dependency  $Sh/Sc^{0.33} = f(Re)$ , obtained from the experimental data.

## 2.3 Calculation of the kinetics and drying efficiency

The drying process effectiveness on the  $i$ -stage of the dryer is presented by the ratio of differences between the moisture contents of the disperse material before and after the drying  $x_{i-1} - x_i$  to the maximum possible (theoretical) difference between the moisture contents on the stage  $x_{i-1} - b_i$  and also in the form of the function of the kinetic parameter of the moisture transfer  $B_i$ , the residence time of

the material on the stage  $\tau_i$ , and the consumption ratio of the dispersed phase to the drying agent  $G_i^{-1}$  [8]:

$$E_i = \frac{\Delta x}{\Delta x_{\max}} = \frac{x_{i-1} - x_i}{x_{i-1} - b_i} = \frac{1 - \exp[-\beta_i \tau_i (1 + G_i^{-1})]}{1 + G_i^{-1}}. \quad (18)$$

### 3. Visualization of results and discussion

#### 3.1 Hydrodynamics

Some graphic dependencies are shown in **Figure 7**. The program receives two- and three-dimensional dependency graphs.

In general dependency diagrams, features for free and constraint motion of particles have one functional dependence. The particle resistance time has enough narrow diapason at every stage (shelf) in free motion regime and is calculated by second units. In the constraint motion regime of particles, the residence time is greatly increased at every stage. The abundant ratio of particles in the two-phase system has a definite impact on this index. That is why, while defining the optimum performance of the device, it is necessary to define the workspace size of the granulating or drying device to high accuracy.

The impact made by some constructive features of the shelf dryer during the residence time of the dispersed material (**Figure 7**) is shown below.

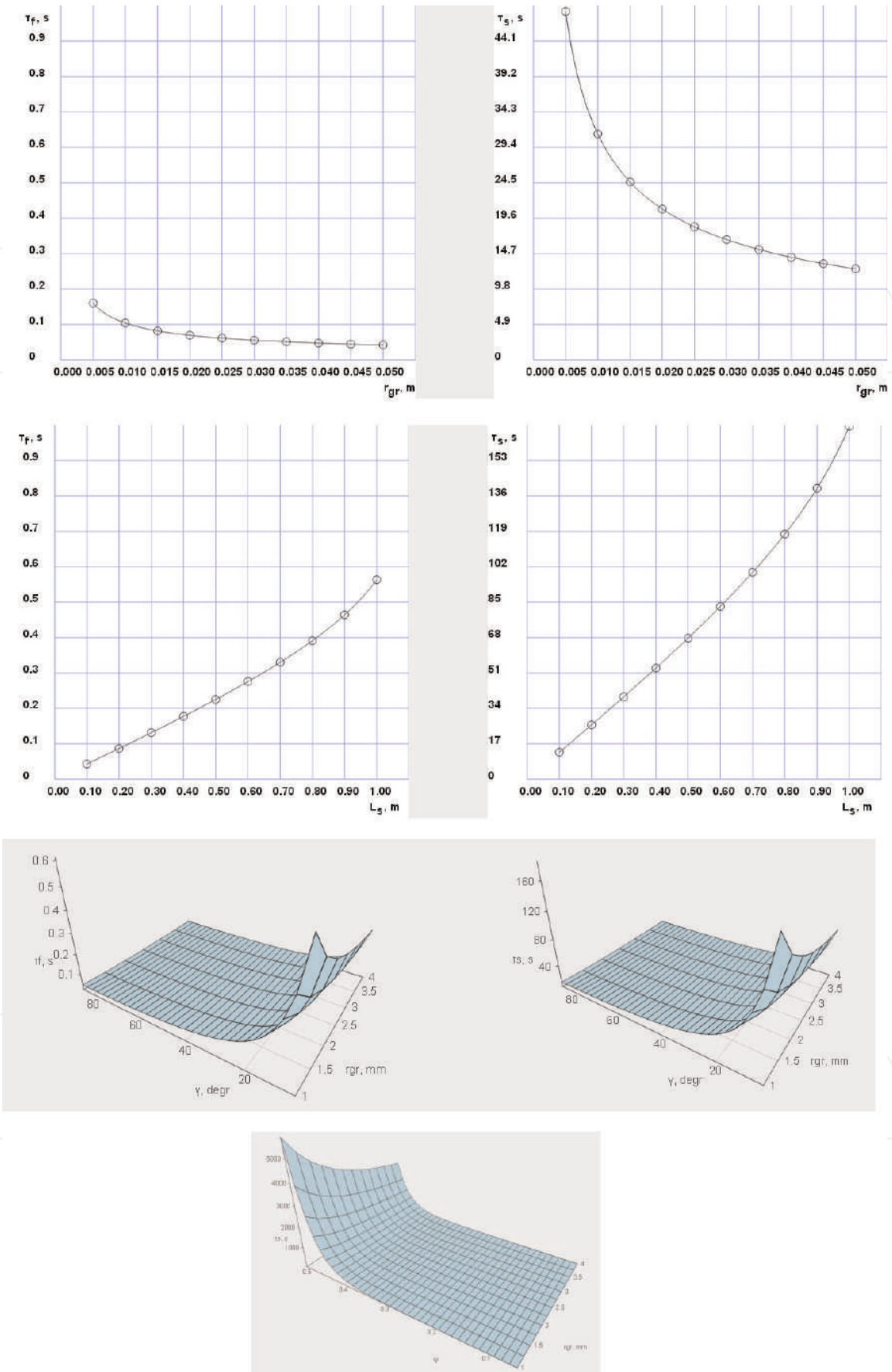
The change of the shelf tilt angle to the horizon affects the redistribution of the gravity components: enlargement of it leads to an increase of the gravity rolling component and vice versa. It should be mentioned that the tilt angle of the shelf may have a minimum value that complies with the natural slope angle of the material. As the tilt angle of the shelf decreases, the residence time of the dispersed material gradually increases. It leads to longer contact with the drying agent's flow.

Changing the gap between the edge of the shelf and the dryer's wall significantly influences the change of the residence time of the dispersed material on the shelf. If the gap increases, the contact time of the dispersed material with the drying agent will be reduced due to the decrease in the length of the material movement distance on the shelf. In this case, the operation of the rolling component of the dispersed material velocity lasts for a shorter period and at the end of the shelf is replaced by the full gravity. Thus, the material moves down, and only the ascending gas flow force resists its fall.

The analysis of the calculations regarding the effect, made by the free cross-sectional area of the shelf on the drying process efficiency, showed the following. Reducing the free cross-sectional area of the shelf leads to an increase of the drying agent's ascending motion velocity in the holes. In this case, the action of the drying agent's ascending flow slows down the progressive motion of the dispersed material on the shelf, compensating for the rolling component of its gravity. The pulse component of the dispersed material displacement decreases, and the trajectory changes to a pulse-forward one. The trajectory length of the dispersed material motion increases, the time of its contact with the drying agent is extended.

As the diameter of the perforation holes decreases, the effect of the drying agent's ascending flow increases, in which the pulse component of the dispersed material motion trajectory decreases, and the forward increases. Thus, the trajectory length of the dispersed material motion increases, and the contact time with the drying agent is extended. It should be noted that with the further reduction of the perforation hole diameter, the action of the drying agent's ascending flow begins



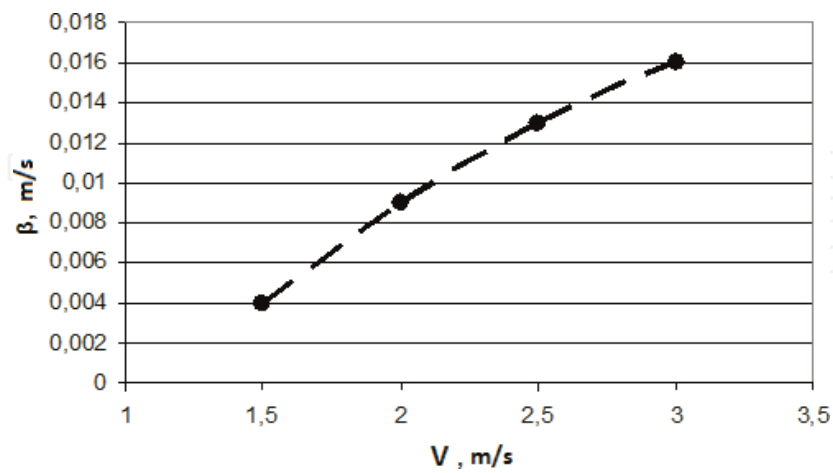


**Figure 7.**  
Examples of calculation results.

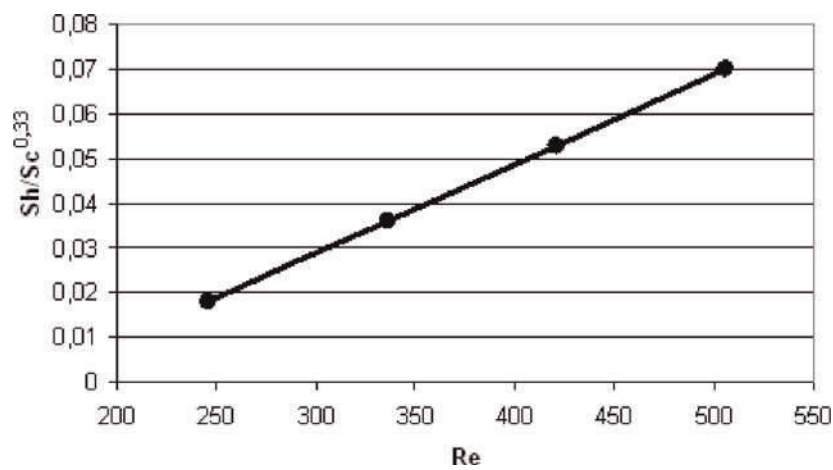
significantly to outweigh the effect of the gravity rolling component. It leads to the formation of the second transitional mode and the ablation mode in the shelf dryer's operation.

3.2 Heat-mass transfer

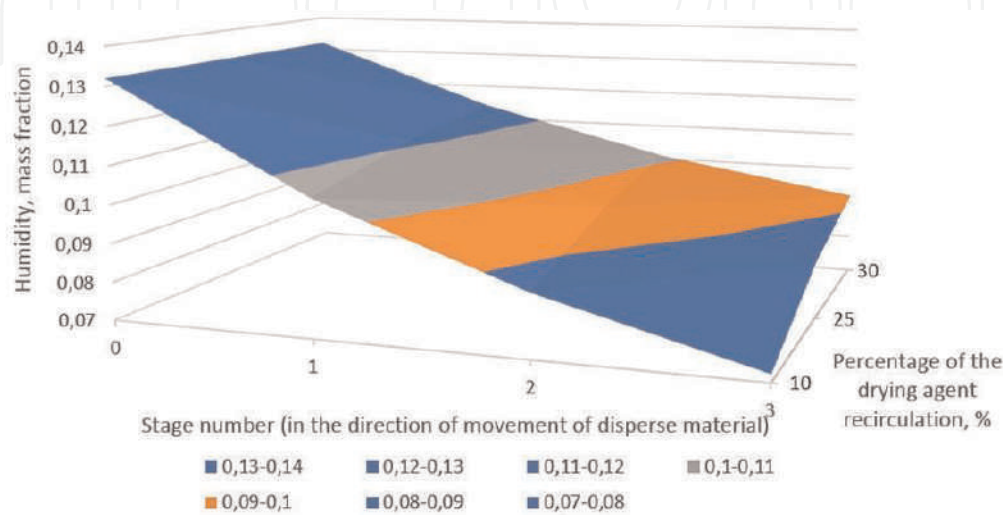
The calculated values of the mass transfer coefficient  $\beta$  from Eq. (16) depending on the velocity of the drying agent's motion are demonstrated in **Figure 8**.



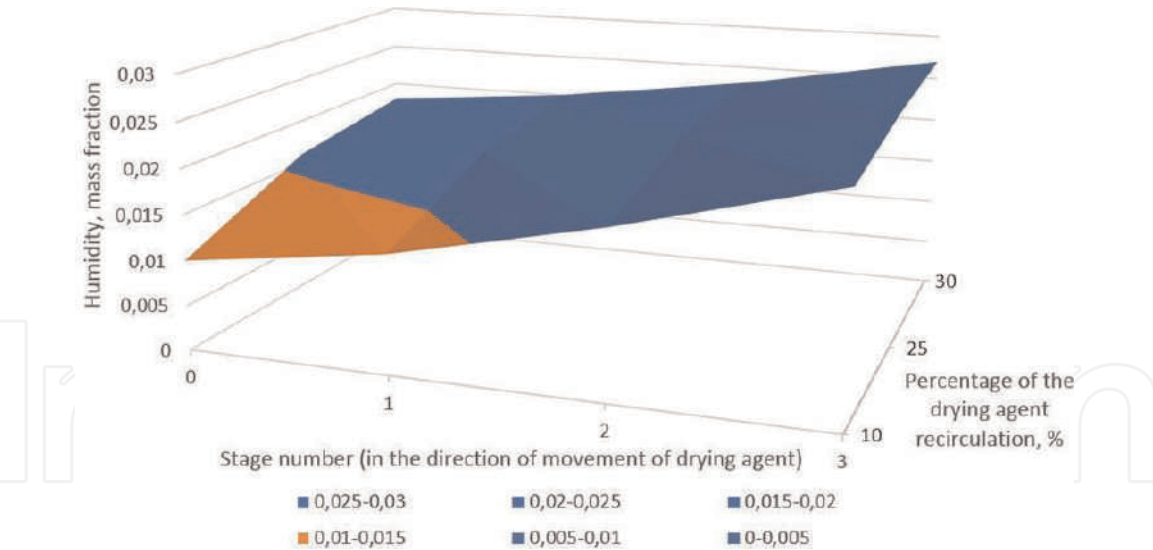
**Figure 8.**  
Dependence of the mass transfer coefficient on the drying agent's motion velocity.



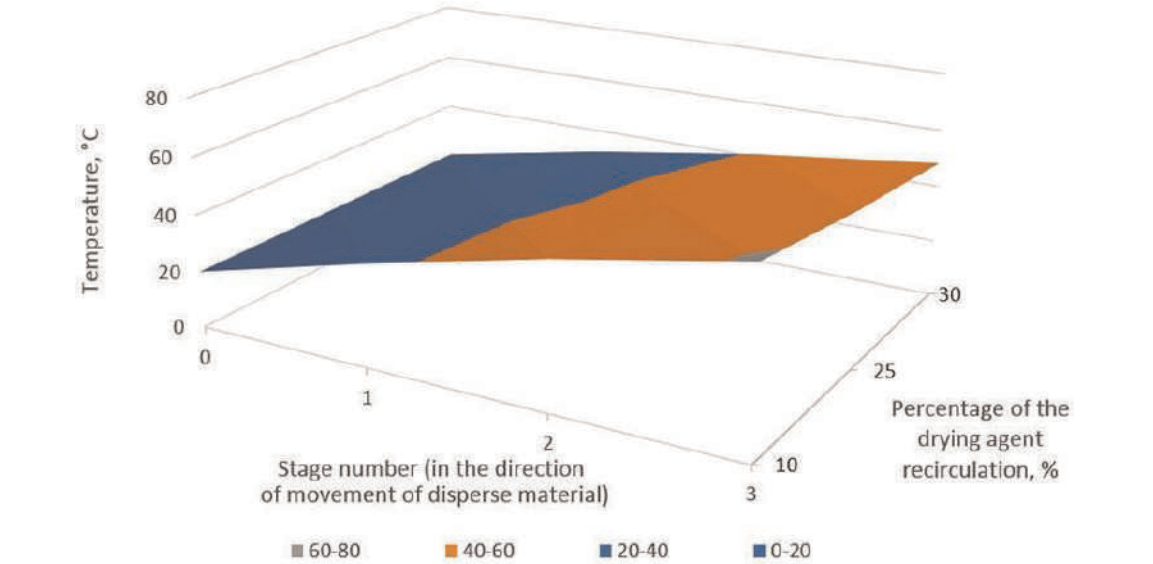
**Figure 9.**  
Graphical dependency  $Sh/Sc^{0.33} = f(Re)$  to define the coefficient  $A_1$  and equation stage  $m$ .



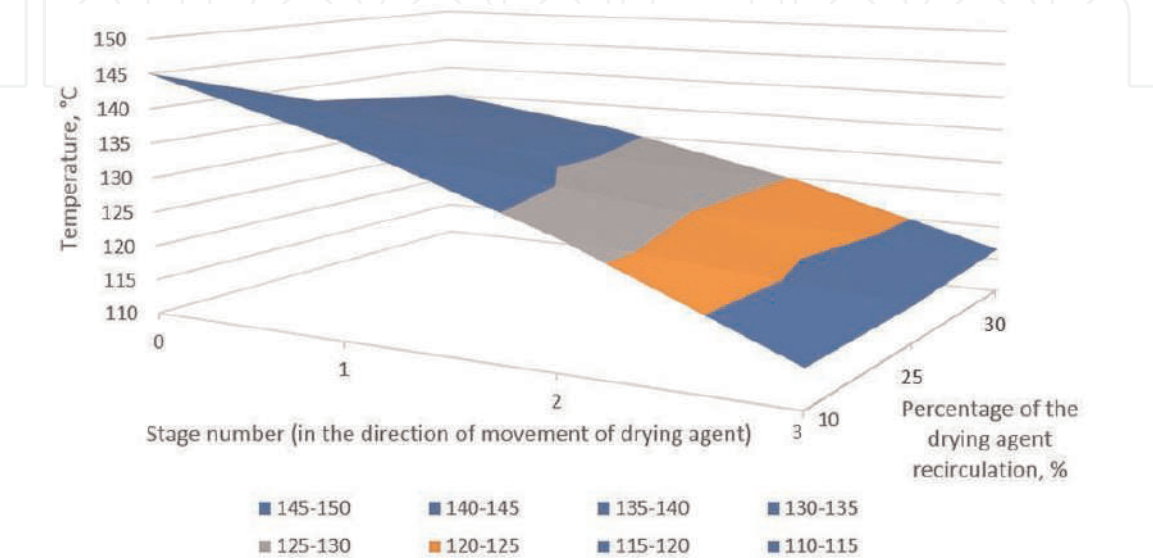
**Figure 10.**  
Influence of the drying agent recirculation method on the change of the moisture content in the disperse material.



**Figure 11.**  
*Influence of the drying agent recirculation method on the change of the moisture content in the drying agent.*



**Figure 12.**  
*Influence of the drying agent recirculation method on the temperature change of the disperse material.*



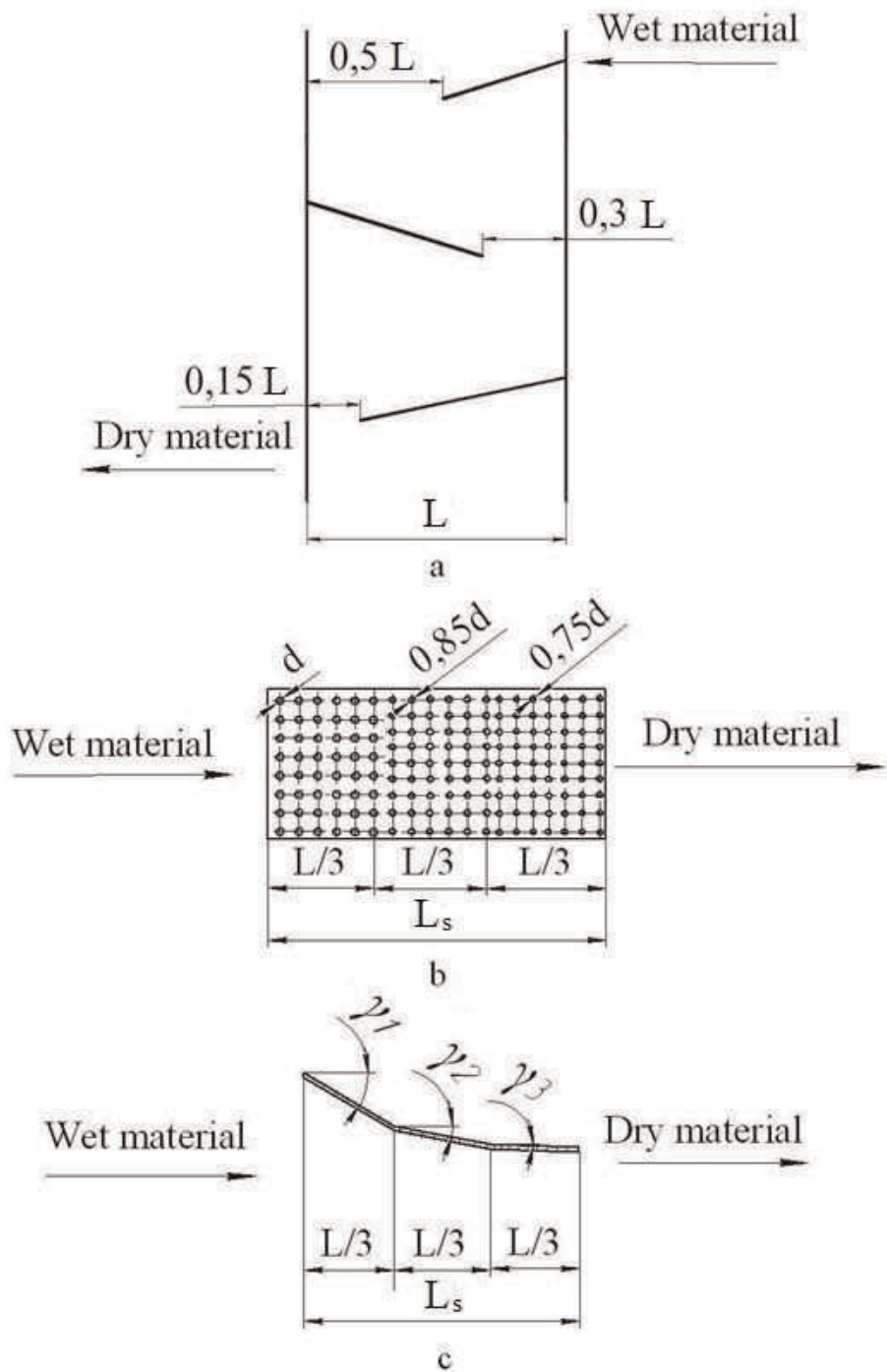
**Figure 13.**  
*An influence of the drying agent recirculation method on the temperature change of the drying agent.*

The graphical dependency from Eq. (17) shows (**Figure 9**) that coefficient  $A_1 = 0.008$ ,  $m = 0.47$ . The coefficient  $n$  is 0.33 for the situation when the drying agent's parameters were slightly changed during the experiment [8].  
Taking into account the obtained values of the coefficient  $A_1$  and equation stage  $m$ , the criterial value (18) will be as follows:

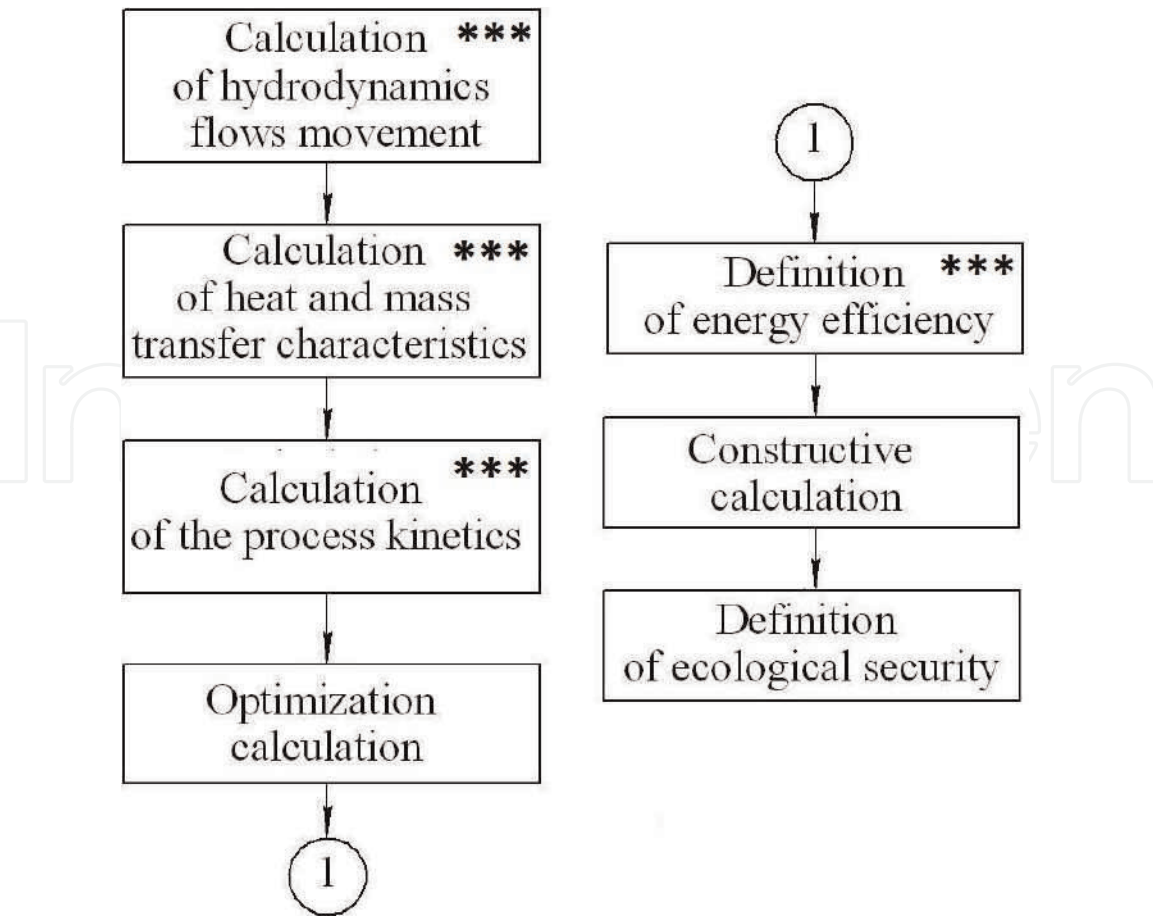
$$Sh = 0.008 \cdot Sc^{0.33} \cdot Re^{0.47} \tag{19}$$

3.3 Kinetics and drying efficiency

The organization of the drying agent's motion may have a considerable influence on the quality indicators of the dried material and the properties of the drying



**Figure 14.** Constructions of shelves in the multistage gravitational shelf dryer [13–15]: (a) shelf with a different gap on the height of dryer, (b) sectioned shelf with variable perforation of sections, and (c) partitioned sections shelf with constant perforation and variable angle of inclination.



**Figure 15.**  
*Block scheme of the algorithm to calculate the multistage gravitational shelf dryer (symbol \*\*\* shows the blocks which are described in this work).*

agent. That has evolved several studies, the results of which are presented in **Figures 10–13**. Their analysis enables us to select the method to organize the drying agent’s motion, which consumes the least energy and ensures the necessary complete removal of moisture from the disperse material.

The analysis of the figures shows that the features of the dispersed material and the drying agent are changed according to one law; each of the technological indicators in the drying agent differently influences the intensity of the increase or decrease of parameters. The figures show that there is no function extremum on the graphical dependencies, which is explained by the regularities of the convective drying kinetics—the parameters’ change of the contacting flows in each of the periods occurs monotonically with different intensity on separate sites depending on the dehydration conditions.

Different constructions of the shelves (**Figure 14**) enable us to control the residence time of the dispersed phase in the dryer’s workspace.

Block scheme of the algorithm to calculate the multistage gravitational shelf dryer is represented in **Figure 15**.

#### 4. Experimental research and practical implementation

During the optimization calculations, the necessity to obtain certain empiric dependencies has been revealed. They would identify some quantities, especially important for the shelf dryer’s design development.

The experimental investigations were carried out on a shelf dryer model, the design parameters of which corresponded to the picture in **Figure 1**. Experiments to



study the properties of the two-phase flow hydrodynamics in a shelf device were carried out at gas flow velocity of 1–5 m/s, specific capacity on the source material 6–10 kg/(m<sup>2</sup> s).

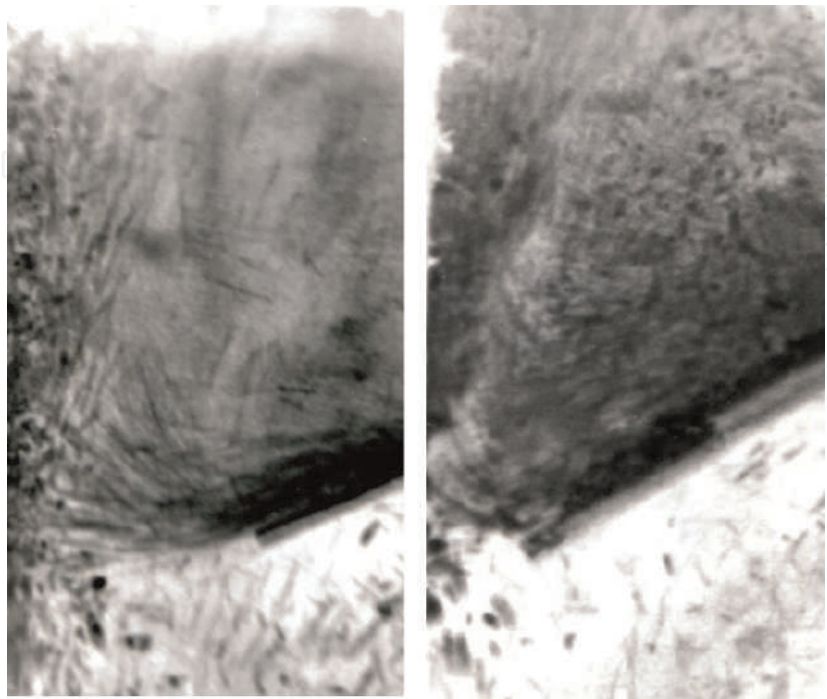
At low gas flow velocities of 0.5–1 m/s, particles of the material move along the surface of the sloping shelf at a velocity of 0.2–0.3 m/s in the form of a rapidly “skipping” layer. The particles of the material are braked at the wall of the device in the discharge space and are accumulated on the surface of the wall (**Figure 16a**) after moving over the surface of the shelf. This accumulated layer is blown by a gas jet, which is formed by a discharge gap between the lower end of the shelf and the wall of the device. As the gas flow velocity increases to 2.5–4 m/s, the porosity of the layer decreases to 0.75–0.8, and the concentration of particles in the layer increases to 40–50 kg/m<sup>2</sup> s.

Small particles, in which the inertia force during their discharge from the surface of the sloping shelf is insufficient to overcome the kinetic energy of the gas jet, are picked up by the jet and move along a curved path to the upper part of the device—the separation zone. On the photo (**Figure 16a**), it is seen by the distinct tracks of the trajectory. Large particles, overcoming the aerodynamic drag of the gas jet, fall out of the layer through the discharge space down. The described hydrodynamic regime is called “gravitationally falling layer.” This mode is implemented on the shelves, installed with a width of the discharge gap (0.3–0.5) L and a free area of 5–10%. Therefore, the maximum efficiency of small fraction ablation by the gas flow is achieved (**Figure 17**). The velocity of the complete ablation of the small fraction without large particles in it—the second critical velocity—is as follows:

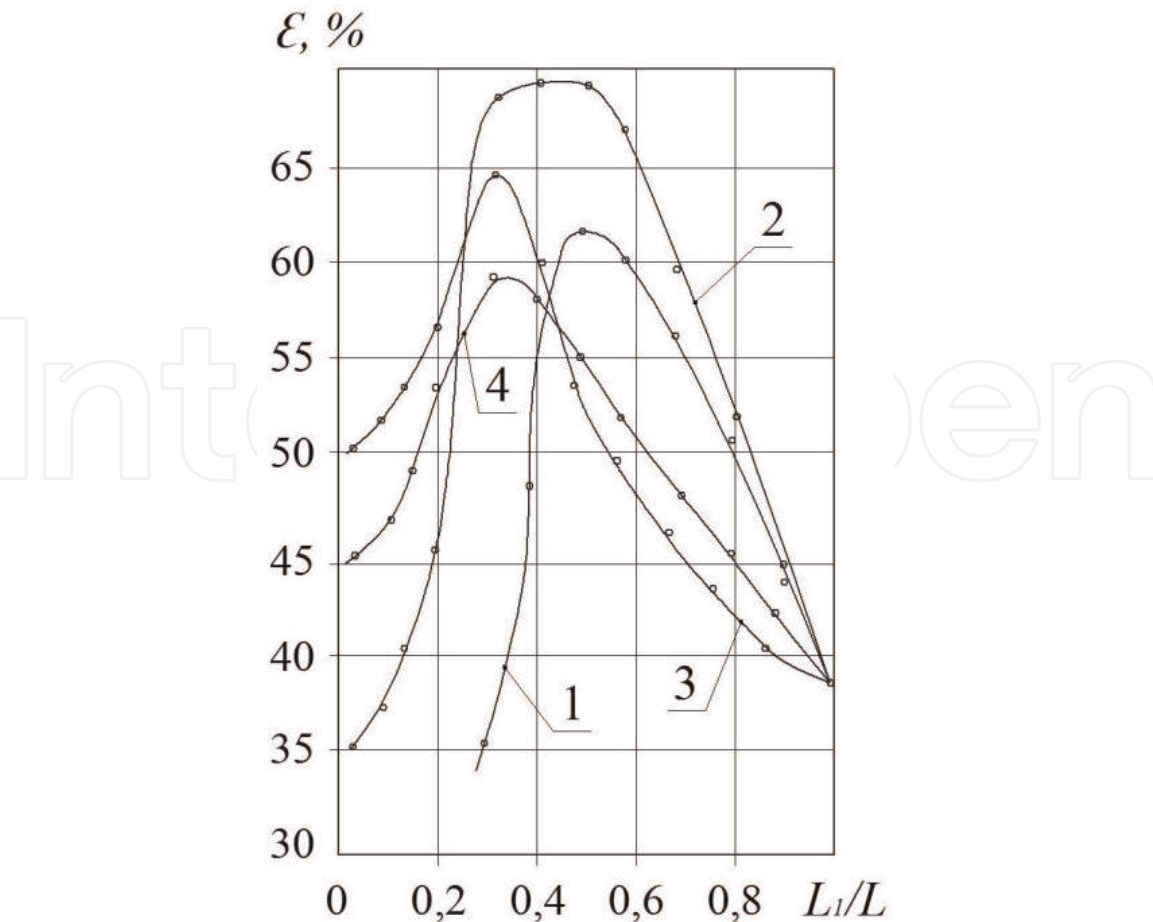
$$Re_{2cr} = 0.1Ar^{0.7}, \text{ with } Ar \leq 62,000, \quad (20)$$

$$V_{cr} = \frac{Re_{2cr} \cdot \nu}{d_{gre}} \quad (21)$$

where  $Ar$  is the Archimedes criterion,  $Ar = \frac{d_{gre}^3 \cdot (\rho_{gr} - \rho_g) \cdot g}{\nu^2 \cdot \rho_g}$ .



**Figure 16.**  
The photo of the hydrodynamic modes of the shelf dryer: (a) “gravitationally falling layer” regime and (b) “weighted layer” regime.



**Figure 17.** The influence of the design (constructive) parameters of the shelf on the extraction efficiency of the fraction less than 1 mm. The free area of the shelf: 1–4, respectively, 0, 5, 15, and 30%. The tilt angle of the shelf is 30°. Material is a polydisperse mixture of the granular superphosphate.

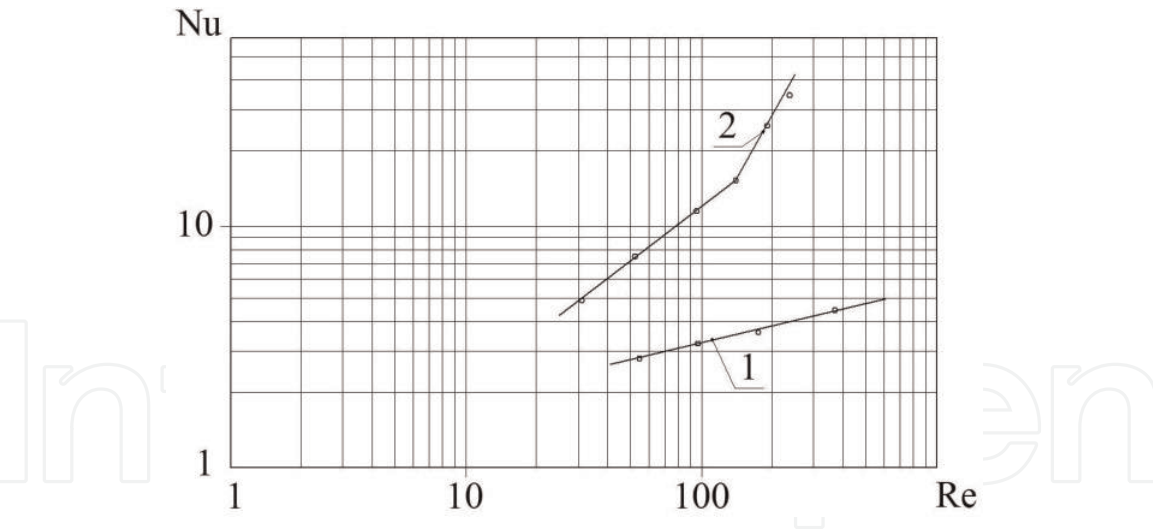
Reducing the width of the discharge space up to (0.15–0.2) L and increasing the free area of the shelf up to 15%, owing to the growing kinetic energy of the gas jet, the continuously circulating vortex layer of particles above the sloping shelf surface is formed (**Figure 16b**). Therefore, the particles of the material are moving on the surface of the sloping shelf in the form of the tightened (compressed) layer at the velocity of 0.05–0.15 m/s, and in the area above, the discharge space—in the form of weighted, intensively circulating layer. The porosity of this layer is 0.65–0.7 (coincides with fluidized systems’ porosity), and concentration of the particles in the workspace of the device is 160–280 kg/m<sup>3</sup>. The described hydrodynamic regime is called the “weighted layer.” The velocity at which the “weighted layer” mode is implemented—the critical velocity when the weighting is started is calculated as follows:

$$R_{wl} = Re_w \cdot k \cdot (L1/L), k = 1.19 \cdot \lg (100 \cdot f_a) + 0.005, \quad (22)$$

$$V_{wl} = \frac{Re_{wl} \cdot \nu}{d_{gre}}, \quad (23)$$

where  $Re_w$  is the Reynolds criterion for particle staying in the gas flow,  $Re_w = \frac{V_w \cdot d_{gre}}{\nu}$ ;  $V_w$  is the velocity of the medium-size particle hovering;  $f_a$  is the free area of the shelf (%).

The effect of the gas flow velocity on the intensity of the interphase heat transfer process is represented by the dependence of the Nusselt criterion on the Reynolds



**Figure 18.** Influence of the gas flow velocity on the interphase heat transfer intensity: (1) “gravitationally falling layer” mode, shelf parameters:  $L_1/L = 0.5$ ;  $f_a = 5\%$ ; (2) “weighted layer” mode, shelf parameters:  $L_1/L = 0.15$ ;  $f_a = 15\%$ .

criterion— $Nu = f(Re)$  (**Figure 18**). These dependencies are described with the following criteria equations:

“gravitationally falling layer mode” $Nu = 1.5 \cdot Re^{0.21}, \tag{24}$

“weighted layer” mode  $Nu = 0.38 \cdot Re^{0.73}. \tag{25}$

Equations (24) and (25) are valid for  $0 \leq Re \leq 500$ .

The above dependencies in the “weighted layer” mode show that the values of the Nusselt criterion are significantly higher than values, which are peculiar for the “gravitationally falling layer” mode. The sufficiently high intensity of heat and mass transfer processes in the “weighted layer” mode is explained by the fact that in this mode the gas jet entering the weighted layer through the discharge gap at sufficiently high velocity has the greatest intensifying effect. Measures of the single-phase flow velocity, carried out by a thermal anemometer in the intersection above the shelf, showed that at gas jet velocities in the discharge space of 6–12 m/s, local heat transfer coefficients at the site of material particles contact with the gas jet are 400–500 W/(m<sup>2</sup> K). These values are peculiar for the intensive heat transfer conditions in the core of the spouting layer and exceed the average heat transfer coefficients for fluidized beds (100–400 W/(m<sup>2</sup> K)) and the pneumatic transportation mode (100–200 W/(m<sup>2</sup> K)).

The rapid evaporation of moisture in the zone above the discharge space leads to some temperature drop of the hot gas before it contacts with the main layer of particles, weighted above the shelf. Experimental studies show that the heating temperature of particles in the zone of contact with the gas jet entering the discharge gap is 1.5–2.0 times higher than that in a weighted layer on the surface of the shelf. It uses a drying agent with higher inlet temperature (1.5–1.8 times higher than melting temperature) than it is acceptable for dryers of the fluidized bed, without fear of the thermal damage of particles.

The investigated construction of the shelf dryer was tested when drying the fine- and coarse-crystalline potassium chloride, sodium pyrosulfite, iron, and nickel powders (**Table 1**).

The shelf dryer, where experimental tests were carried out, is a vertical rectangular-sectioned shaft, inside which the sloping perforated shelves are located in cascade on opposite sides (**Figure 1**). Wet material is fed by the batcher to the

| Material                        | The velocity of the drying agent, m/s | Humidity, % wt  |               |          | Moisture removal intensity, kg/(m <sup>3</sup> h) |
|---------------------------------|---------------------------------------|-----------------|---------------|----------|---|
|                                 |                                       | Source material | Undershooting | Ablation |   |
| Fine-coarse potassium chloride: | 1.32                                  | 6.1             | 0.35          | 0.24     | 421   |
|                                 | 1.5                                   | 6.1             | 0.1           | 0.06     | 462   |
|                                 | 1.45                                  | 8.0             | 1.2           | 0.2      | 1025  |
|                                 | 1.9                                   | 7.0             | 0.1           | 0.17     | 527   |
|                                 | 2.1                                   | 8.0             | 0.11          | 0.1      | 1173  |
| Coarse-crystalline              | 2.3                                   | 7.0             | 0.14          | 0.1      | 528   |
|                                 | 2.8                                   | 5.0             | 0.5           | 0.1      | 250   |
|                                 | 3.3                                   | 5.0             | 0.5           | 0.1      | 346   |
|                                 | 3.5                                   | 6.0             | 0.6           | 0.2      | 258   |
| Sodium pyrosulfite              | 2.0                                   | 10.0            | 0.34          | 0.3      | 1826  |
| Iron powder                     | 2.3                                   | 11.3            | 0.4           | 0.3      | 600   |
| Nickel powder                   |                                       |                 |               |          |   |

**Table 1.**  
*Results of the drying of the granular materials in the shelf dryer.*

upper shelf, is weighed above it, and is divided into small and large fractions. The upper shelf works in the hydrodynamic regime of the “gravitationally falling layer.” In this mode, the dedusting process of materials, i.e., the removal of small particles from the initial mixture by the minimum interface, is effectively carried out. The minimum interface for shelf devices is 50–70 μm. The small particles are carried away by the drying gas agent into the separation space and then captured by a cyclone in which they are dried. Large particles fall down through the discharge space to the lower shelf.

When drying the materials, which are prone to the formation of lumps and strongly sticking to surfaces, the distance from the delivery point of the wet product into the device to the upper shelf has to be at least 0.3–0.5 m. The material, passing this distance, breaks up into small pieces and is partially dried. A hydrodynamic regime of the “weighted layer” is created on the lower shelf, in which, due to the intensive circulation and mixing of particles in the layer, the drying process is effectively carried out. The longer residence time of the particles in this layer also contributes to it.

The wet material, discharged from the upper shelf, enters the lower shelf from the top of the weighted layer, is drawn into the circulation, and is dried quickly. The share of the dried material falls through the discharge space into the hopper, in which a large fraction of the dried product is collected.

Thanks to the shelf contact elements, shown by the data of **Table 1**, the drying process takes place at the drying agent’s moderate velocities (maximum 3.5 m/s) and at a large moisture intensity of the dryer’s workspace which is up to 1000–1500 kg/(m<sup>3</sup> h). Due to the intensive contact between phases in the shelf devices, the drying process is carried out at high specific loads of up to 15–20 kg/(m<sup>2</sup> s), significantly exceeding the specific loads of 0.1–1.5 kg/(m<sup>2</sup> s) for fluidized bed devices. The specific consumption of the drying agent in the shelf dryers reaches



0.5–0.7 m<sup>3</sup>/kg, and the hydraulic resistance is 1300–1500 Pa, respectively, against the values of 1.4–2.8 m<sup>3</sup>/kg and 1800–2200 Pa for fluidized bed devices. The working path of the pneumatic pipe dryer, in which energy is expended to accelerate and to lift the drying material, has a hydraulic resistance of 1600–2000 Pa.

An additional advantage of shelf dryers is the simultaneous dedusting of the drying material. Fine-crystalline potassium chloride, containing 7–10% of the small fraction with a particle size of less than 100 µm in the initial mixture, after processing in a shelf device at a gas flow velocity of 1.4–1.5 m/s, had 1.2–5.5% of the small fraction in the final product (undershooting) and 60–80% of the small fraction in ablation. Coarse-crystalline potassium chloride, containing 4–10% of the small fraction with a particle size of less than 100 µm in the initial mixture, had 2–5% of the small fraction in the final product (undershooting) at a gas flow velocity of 1.3–1.4 m/s and 58–65% of the small fraction in the ablation. The extraction degree of the small fraction into the ablation was 70–90%. When the gas flow velocity exceeds 1.5 m/s in the final product, the small fraction is practically absent, and the content of the coarse fraction (more than 100 µm) in ablation is 3–5%.

The small fraction was completely extracted from the polydisperse mixture of granulated superphosphate containing up to 20% of the small fraction with particle sizes less than 1 mm, after processing in the shelf device at a gas flow velocity of 3.5–3.8 m/s, into the ablation. Therefore, the extraction degree of the small fraction into ablation was 80–85%.

In order to prevent the coarse fraction ablation by the gas flow and increasing the residence time of particles in the separation space for drying the ablative fractions, the upper section with a constant intersection was replaced with a conical free intersection [16] or with shelf contact elements [17].

Thus, the shelf dryers achieve the higher technological effect than typical constructions of the fluidized bed dryers and pneumatic pipe dryers, with less energy, capital costs, and sizes.

## 5. Conclusions

The convective shelf dryer construction with active aerodynamic processing modes is proposed. The developed engineering method for the shelf dryer calculation made it possible to define the constructive parameters of the device, ensuring the minimum required drying time of the wet material in the device to a predetermined humidity index. The demonstrated author's program Multistage Fluidizer® for computer implementation of the engineering calculation method made it possible to optimize the constructive and operating parameters of the drying process in the shelf device. It was shown that a shelf dryer should have, for example, three shelf contacts with various widths of the discharge space and various free areas of the shelves.

The author shows various hydrodynamic regimes to weigh particles of a material by a gas flow, depending on the constructive parameters of shelf contacts.

The effectiveness of the shelf device to carry out the drying and dedusting processes of granular and powder materials simultaneously was experimentally proven.

## Acknowledgements

This research work has been supported by the Slovak Grant Agency VEGA Grant No. 1/0731/16 "Development of Modern Numerical and Experimental



Methods of Mechanical System Analysis,” by Cultural and Educational Grant Agency of the Slovak Republic (KEGA) Project No. KEGA 002TnUAD-4/2019, and by the Ministry of Science and Education of Ukraine under the project “Small-scale energy-saving modules with the use of multifunctional devices with intensive hydrodynamics for the production, modification and encapsulation of granules,” Project No. 0119U100834.

### **Conflict of interest**

The authors declare that they have no competing interests.

### **Author details**

Artem Artyukhov<sup>1\*</sup>, Nadiia Artyukhova<sup>1</sup>, Ruslan Ostroha<sup>1</sup>, Mykola Yukhymenko<sup>1</sup>, Jozef Bocko<sup>2</sup> and Jan Krmela<sup>3,4</sup>

<sup>1</sup> Sumy State University, Sumy, Ukraine


<sup>2</sup> Technical University of Košice, Košice, Slovak Republic

<sup>3</sup> Alexander Dubcek University of Trencin, Puchov, Slovak Republic

<sup>4</sup> University of Pardubice, Pardubice, Czech Republic

\*Address all correspondence to: a.artyukhov@pohnp.sumdu.edu.ua

### **IntechOpen**

© 2019 The Author(s). Licensee IntechOpen. This chapter is distributed under the terms of the Creative Commons Attribution License (<http://creativecommons.org/licenses/by/3.0>), which permits unrestricted use, distribution, and reproduction in any medium, provided the original work is properly cited. 

## References

- [1] Delgado JMPQ, Barbosa de Lima AG, editors. *Transport Phenomena and Drying of Solids and Particulate Materials*. Switzerland: Springer International Publishing; 2014. 115p
- [2] Kowalski SJ, editor. *Drying of Porous Materials*. Netherlands: Springer; 2007. 231p
- [3] Sazhin BS, Sazhin VB. *Scientific Principles of Drying Technology*. USA: Begell House Publishers Inc.; 2007. 509p
- [4] Kowalski SJ. *Thermomechanics of Drying Processes*. Germany: Springer-Verlag Berlin Heidelberg; 2003. 358p
- [5] Delgado JMPQ, Barbosa de Lima AG, editors. *Drying and Energy Technologies*. Switzerland: Springer International Publishing; 2016. 228p
- [6] Mujumdar AS, editor. *Handbook of Industrial Drying*. 4th ed. USA: CRC Press Taylor & Francis Group; 2014. 1348p
- [7] Law CL, Azharul K, editors. *Intermittent and Nonstationary Drying Technologies: Principles and Applications*. 1st ed. USA: CRC Press Taylor & Francis Group; 2017. 244p
- [8] Artyukhova NA, Shandyba AB, Artyukhov AE. Energy efficiency assessment of multi-stage convective drying of concentrates and mineral raw materials. *Naukovyi Visnyk Natsionalnoho Hirnychoho Universytetu*. 2014;**1**:92-98
- [9] Artyukhov AE, Sklabinskyi VI. Experimental and industrial implementation of porous ammonium nitrate producing process in vortex granulators. *Naukovyi Visnyk Natsionalnoho Hirnychoho Universytetu*. 2013;**6**:42-48
- [10] Kudra T, Mujumdar AS. *Advanced Drying Technologies*. 2nd ed. USA: CRC Press; 2009. 438p
- [11] Artyukhova NA. Multistage finish drying of the  $N_4HNO_3$  porous granules as a factor for nanoporous structure quality improvement. *Journal of Nano- and Electronic Physics*. 2018;**10**(3): 03030-1-03030-5
- [12] Artyukhov AE, Artyukhova NO, Obodyak VK, Horishnyak AO. Certificate of authorship No. 79141 (Ukraine). Computer program Multistage Fluidizer©
- [13] Artyukhova NO, Yukhymenko MP, Artyukhov AE, Shandyba AB. Patent No. 74070, (Ukraine). Device for drying of disperse materials
- [14] Artyukhova NO, Yukhymenko MP, Artyukhov AE, Shandyba AB. Patent No. 81720, (Ukraine). Device for drying of disperse materials
- [15] Artyukhov AE, Artyukhova NO, Shandyba AB. Patent No. 92423, (Ukraine). Device for drying of disperse materials
- [16] Yukhymenko M, Ostroha R, Litvinenko A, Bocko J. Estimation of gas flow dustiness in the main pipelines of booster compressor stations. *IOP Conference Series: Materials Science and Engineering*. 2017;**233**:012026
- [17] Lytvynenko A, Yukhymenko M, Pavlenko I, Pitel J, Mizakova J, Lytvynenko O, et al. Ensuring the reliability of pneumatic classification process for granular material in a rhomb-shaped apparatus. *Applied Sciences*. 2019;**9**:1604